Food web structure and biogeochemical processes during oceanic phytoplankton blooms: An inverse model analysis.

Robert M. Daniels[a], Tammi L. Richardson[b,c] and Hugh W. Ducklow[a,*],

[a]*The College of William and Mary, School of Marine Science, P.O. Box 1346, Gloucester Point, VA 23062, USA. Fax: (804)684-7293*

[b]*Department of Oceanography, Texas A & M University, College Station, TX, 77843-3146, USA*

c Current address: Marine Sciences Program, Dept. of Biological Sciences, University of South Carolina, Columbia, SC 29208

** corresponding author*

Deep-Sea Research II
(submitted 03 May, 2004)
(revised 11 July, 2005)

Abstract

The relationship between food web structure and function across two ocean biomes was investigated using an inverse method to recover solutions of food web carbon flows. We estimated the carbon exchanges between major assemblages within plankton food webs in the North Atlantic, using the JGOFS NABE data set (1989) and near the Western Antarctic Peninsula (WAP), using the Palmer Station LTER data set, two areas exhibiting strong seasonal phytoplankton blooms. The recovery of all the potential flows of carbon allowed a system level analysis, providing insight to processes that are seldom measured in the field and a means of comparing food webs from different regions. In the NABE food web, the dominant carbon flows involved the microorganisms including bacterial carbon demand and grazing by microzooplankton and protozoans. In the WAP food web, krill had the most significant carbon flows including grazing of large phytoplankton and respiration.

A comparison between the NABE and the WAP carbon–based food webs showed key differences. Recycling and the activity of the microbial food web were much greater in the NABE food web than in the WAP. However in the WAP inverse solution, the microbial food web was just as important as the classical food web (diatoms to krill to penguins) that is traditionally believed to dominate carbon flows. Carbon flows through the NABE and WAP regions were more highly dependent on recycling than would be anticipated from the size structure of the primary producers, when analyzed using a classification scheme of Legendre and Rassoulzadegan (1996).

1. Introduction

Biological oceanographers traditionally pursue information about individual taxonomic or functional groups at varying levels of specificity (e. g., "phytoplankton," "diatoms," "*Nitzschia spp*," "mesozooplankton," "copepods," "*Calanus*"). It remains technically challenging to specify the biomass and key rate processes of aggregated groups, much less pertinent information for key species groups. Even less emphasis has been directed toward holistic, systems-level understanding of the composition and functioning of plankton ecosystems. Beyond a few descriptive syntheses (e. g., Landry et al., 1997; Niquil et al., 1998; Garrison et al., 2000) such efforts mostly involve numerical simulation modeling at low to moderate levels of trophic resolution (Fasham, 1995). Inverse food web modeling is an alternative approach, ideal for exploring the potential value hidden in observational data (Vézina and Platt, 1988). Here, we continue a systematic effort to explore the connections between food web structure and biogeochemical processes in plankton systems and in biogeochemical provinces studied by JGOFS and other programs in the past decade (Ducklow 2003; Richardson et al., 2004).

Ocean environments in different regions of the world have different food web structures that have adapted to the regional circulation and climate conditions (Lochte et al., 1993; McCarthy et al., 1996; Longhurst, 1998; Karl, 1999a). Thus upwelling regions are typically characterized by short or 'classical' food webs consisting of three main trophic levels: large phytoplankton, mesozooplankton grazers, and fish (Ryther, 1969), with high f-ratios and high export. Oligotrophic gyres have more complex food webs consisting of small phytoplankton, protozoans, microzooplankton, mesozooplankton grazers, and finally fish (Karl, 1999a). For example, the North Pacific Subtropical Gyre (NPSG) is considered to be a "microbial

ecosystem" dominated by prokaryotic autotrophs that are grazed upon by active protozoan and microzooplankton communities (Karl, 1999a). High latitude systems are typically characterized by short food chains dominated by diatom blooms and mismatches between production and grazing (Longhurst, 1995; Pesant et al., 1998).

Important biogeochemical processes influenced by food web structure include particle export, nutrient regeneration, and dissolved organic matter (DOM) production (Michaels and Silver, 1988). Food web structures that promote consumption and retention of organic matter in the upper water column (e.g., small cells, complex feeding relationships) will tend to enhance nutrient regeneration (Carlson et al., 1994) and will result in lower f-ratios at the expense of export. Dissolved organic carbon (DOC) has been shown to play a significant role in export from the surface layer (Carlson et al., 1994) and also is a major resource for bacterial uptake. The lack of knowledge of DOC production and fluxes through the food web presents a significant roadblock to modeling the open ocean microbial food web (Legendre and Gosselin, 1989; Karl, 1999a). The intensity of these processes, and the chemical composition of the fluxes are influenced by the taxonomic composition and size structure of plankton food webs.

Previous researchers have investigated links between food web structure and these key biogeochemical processes. Eppley and Peterson (1979) related the export of particulate organic matter out of the surface ocean to rates of primary productivity in ocean environments with very different food web structures. They calculated f-ratios for regions ranging from the oligotrophic central North Pacific to the highly productive upwelling region off the coast of Peru. The central North Pacific had a low f-ratio of about 0.05, indicating a system dominated by recycling and a relatively high residence time for nitrogen in the surface ocean. In the Peru upwelling region, the

f-ratio was 0.5 with half of the total production fueled by nitrate upwelled from the deep waters. Legendre and Rassoulzadegan (1996) modeled links between food web structure and export, concluding that the flows of biogenic carbon are strongly influenced by the size distribution of the primary production and the matching between primary production and grazing, two key aspects of food web structure. It is not always obvious, however, that export is driven by food web structure. Rivkin et al. (1996) showed that export fluxes were similar in the Gulf of St. Lawrence even when the food webs were very different (microbial vs. herbivorous).

Phytoplankton blooms often dominate ocean biogeochemistry in various ecological provinces (Watson and Whitfield, 1985; Longhurst, 1998). Here we examine the relationships between food web structure and key biogeochemical processes for two systems characterized by conspicuous spring phytoplankton blooms, the North Atlantic Ocean and the Western Antarctic Peninsula (WAP). The JGOFS North Atlantic Bloom Experiment (NABE; Ducklow and Harris, 1993) established that the bloom in this region did not necessarily correspond to the classical idea of a phytoplankton bloom dominated by large cells, having a high f-ratio and displaying mismatches between production and grazing (Garside, 1993; Harrison et al., 1993; Lochte et al., 1993; Martin et al., 1993). Mesozooplankton contributed only a small portion to the total plankton biomass and grazed a small percentage of the primary production (Dam, 1993; 1995) and high microbial activity was observed (Ducklow et al., 1993).

In contrast to NABE, the food web in the western Antarctica Peninsula has only a few links between primary producers and large apex predators (Smith et al., 1998). The shortest path through the food web is from large diatoms to krill (*Euphausia superba*) to the apex predator, the Adélie penguin (*Pygoscelis adeliae)*. Yet some aspects of WAP food webs suggest more

complexity. Although short paths through the food web are available, the microbial food web is present in the Antarctic as it is throughout the world's oceans (Fuhrman, 1989, Karl, 1999b, Pomeroy, 2001). Microbial processes in the Southern Ocean are still poorly understood and not well sampled (Karl et al., 1996).

Our study focused in part on the role of microbial vs classical food webs in these two regions. We used the inverse method (Vézina and Platt 1988) to test the conclusion that the bloom in NABE was not a 'classical' phytoplankton bloom and that the microbial processes were more significant than classical food web processes. For the western Antarctic Peninsula, we set out to better understand the relative role of the microbial food web vs. the classical food web. We compared the results from spring blooms of similar magnitude occurring in very different regions.

2. Methods

We used an inverse method (Vézina and Platt 1988) to describe plankton food web structure in these regions more fully. The inverse method uses observed data to recover estimates of all the flows within a specified food web, many of which are seldom measured. This method has been adapted from the physical sciences (Parker, 1977; Wunsch, 1978; Wunsch and Minster, 1982), where it was used to infer ocean currents from hydrographic data. It has also been adapted to infer stocks of fish species using the program, ECOPATH (Pauly et al., 2000). It was first applied to plankton food webs by Vézina and Platt (1988) for the Celtic Sea and then later by other researchers for a variety of benthic and pelagic systems (e.g. Jackson and Eldridge, 1992;

Eldridge and Jackson, 1993; Vézina and Pace, 1994; Donali et al., 1998; Niquil et al., 1998).

In plankton food webs, as with geophysical problems, the number of unknowns can far outnumber the independent measurements taken. The inverse method works opposite from forward models in that it uses observations of the standing stocks and flows, along with known biological constraints to solve for unknown flows and rate parameters. The inverse method minimizes the sum of squared flows and arrives at a solution that is consistent with real data from the system, satisfies conservation of mass, and obeys the specified biological constraints (Vézina and Platt, 1988).

Carbon was the currency used in the models presented here. The living components (Figure 1) included small and large phytoplankton, bacteria, protozoans, microzooplankton and mesozooplankton (krill in the WAP model). The nonliving components were DOC and detritus. Phytoplankton were nominally split into large (>5 μm) and small (0.2 – 5 μm) size fractions. Legendre and Rassoulzadegan (1996) used these classes to distinguish the smaller phytoplankton that mesozooplankton can't efficiently graze from the larger phytoplankton that they do graze. Also, the large phytoplankton along with other particles >5 μm are more likely to form aggregates and sink to depth. The 'protozoans', as defined here, represented the smallest heterotrophic grazers (<10 μm) including heterotrophic nanoflagellates and ciliates (Capriulo, 1990) that feed upon bacteria and each other. 'Microzooplankton' included heterotrophic organisms between 10–200 μm such as larger nano- and microflagellates, dinoflagellates, ciliates, sarcodines and copepod nauplii (Verity et al., 1993). Heterotrophic organisms greater than 200 μm that can be captured in plankton nets, such as copepods and euphausiids, constituted the mesozooplankton (Vézina and Platt, 1988).

The mesozooplankton were restricted from grazing on the small phytoplankton and bacteria in our food webs (Figure 1). The grazers, including the protozoans, microzooplankton and mesozooplankton were allowed to consume other grazers, as long as their prey were smaller in size. All of the grazers were allowed to consume detritus. All of the living components except bacteria, and also detritus were allowed to contribute to the DOC compartment. Inputs to the system were the gross primary production by large and small phytoplankton. Outputs from the system were sinking detritus, mesozooplankton or krill production, and respiration by the living compartments.

All of the possible flows in the food web were defined by mass balance equations (Appendix A), such that the flows entering each component must equal the flows leaving, plus any observed or assumed change in biomass of the component over the period studied. Steady states are not required. Measured food web flows were used as targets for the solution, and were allowed to vary within one standard deviation of the measured or specified values (Appendix A). The boundary conditions for the model were defined using measured primary production as the input and measured sedimentation as the output for the system (Appendix A). Biological constraints (Appendix B), such as respiration and assimilation efficiency were used to keep the unknown flows within reasonable ecological and physiological boundaries (Jackson and Eldridge, 1992; Vézina and Platt, 1988). For example, the growth efficiency for bacteria was constrained to an upper bound by forcing the bacterial respiration to be greater than or equal to 50% of the bacterial carbon demand (Vézina and Platt, 1988). The inverse solution to the food web flows was found using the same procedure as described in this volume by Richardson et al. (2005).

Sensitivity analysis and various network analysis techniques were used to analyze model results. The input parameters to the models were varied by ± 10% in order to test the sensitivity of the model flows to small changes in the inputs. The sensitivity analysis highlights measurements that the modeled food web is sensitive to, as well as organisms and flows in the model that are sensitive to changes in input and parameter settings.

Models can be analyzed using network analysis techniques that calculate useful statistics about the modeled system that are not obvious, such as the degree of internal cycling within the food web or the effective trophic level of a compartment (e.g., mesozooplankton). The indices used were based on the network analysis approach of Ulanowicz (1986) and the application of network analysis to inverse models by Niquil (1998). The NETWRK program (Ulanowicz 1986), available at www.cbl.cees.edu/ /~ulan/ntwk/network.html, was used to compute network analysis indices based on the model solution flows. Here we show the effective trophic levels for each living and nonliving component. Other indices used were ***F, L,*** and **Total ingestion / PP.** ***F*** is the fractional flow through a specific compartment either divided by the net primary production or the total flows through compartments with a similar trophic level. ***Fbac*** is equal to the ratio of bacterial production to net primary production (Niquil et al., 1998). ***Fpro***, ***Fmic***, ***Fmes,*** and ***Fkri*** are the ratios of the total flows through the protozoan, microzooplankton, mesozooplankton and krill compartments, respectively, to the total flows through all grazer compartments (Niquil et al., 1998). The index of recycling, ***L,*** is an estimate of the average number of times a carbon atom passes through the system before export (Niquil et al., 1998). Another index of recycling, the **Total ingestion / PP** is equal to the sum of all grazer ingestion flows, plus bacterial uptake of DOC, divided by the net primary production.

3. Data Synthesis and Model Inputs

Model solutions are dependent on, and are required to obey observations. Here we provide brief descriptions of the methods used in data collection and processing, necessary for understanding how the model results were constrained and derived. The original publications and Daniels (2003) should be consulted for further details. The North Atlantic model included the basic components described above and shown in Figure 1a. The western Antarctic Peninsula model (Figure 1b) includes the same components as in the North Atlantic model, except that krill were the only mesozooplankton grazer represented because they are usually the dominant zooplankter in the area (Ross et al., 1996).

3. 1. North Atlantic Bloom Experiment (NABE)

The majority of the data for the NABE food web were taken from the May 18 –31, 1989 US JGOFS cruise on the RV Atlantis II, during the later phase of the still-active bloom. This period has the most inclusive data for the study, including in many cases daily measurements of phytoplankton production and biomass, new and regenerated production, bacterial production and biomass, microzooplankton grazing and biomass, mesozooplankton grazing and biomass, and export. Data were downloaded from http://usjgofs. whoi. edu/jg/dir/jgofs/nabe/atlantisII/ and are also available on the United States JGOFS Process Study Data 1989-1998 CD-ROM, (available from US JGOFS Office, WHOI). The measurements were integrated to 35 m, the depth of ^{234}Th-based estimates of export (Buesseler et al., 1992). Carbon measurements were averaged over the two-week observation period to arrive at mean values to be used in the inverse analysis (Table 1). The standard deviations of the daily integrated rate measurements were used

to set minimum and maximum constraints on these flows. In cases where the standard deviation was not available, we chose wide ranges (e.g., 0.5 to 1.5 times the measured values) in order to avoid forcing the model into a particular result.

Regressions were performed on the biomass measurements vs. time to determine if there were significant changes over the study period. Bacterial biomass increased by 6.3 mmol C m^{-2} d^{-1} and microzooplankton biomass increased by 9.2 mmol C m^{-2} d^{-1} (Figure 2). These changes were entered into the balance equations for bacteria and microzooplankton (Appendix A), respectively, forcing the model to account for the observed increases in these compartments.

Primary production (Figure 2) was measured *in situ* approximately every other day (Martin et al., 1993). The average primary production integrated to 35 m was 88 mmol C m^{-2} d^{-1}, nearly equal to the production integrated to the depth of the entire euphotic zone (35-50 m) of 91 mmol C m^{-2} d^{-1} (Martin et al., 1993). The average primary production was split evenly between the small and large phytoplankton (Joint et al. 1993). Phytoplankton biomass (Figure 2) was estimated from Chl a (Repeta, 2003) using a C:Chl a ratio of 80 (Ducklow et al., 1993). Bacterial production was estimated by Ducklow et al. (1993) using ^{3}H-thymidine incorporation. Bacterial biomass was estimated daily from acridine orange direct counts (Figure 2). Dilution experiments were performed 3 times to provide grazing rates for zooplankton smaller than 200 μm, including both the protozoan and microzooplankton size classes in the models (Verity et al., 1993). Total microzooplankton biomass (Figure 2) was derived from measurements of abundance and group specific biomass of ciliates, dinoflagellates, and microflagellates (Verity et al., 1993). Dam et al. (1993) estimated the total mesozooplankton grazing using gut fluorescence and gut clearance experiments for mesozooplankton split into three size classes: 0.2 – 0.5 mm, 0. 5 – 1. 0 mm, and

1.0 – 2. 0 mm (Figure 2). Mesozooplankton carbon biomass (Figure 2) was measured independently from trawls (Dam, 1993). The export from the NABE system was estimated from measurements of ^{234}Th: ^{238}U disequilibria (Buesseler et al., 1992) reported as both low and high estimates of carbon flux at 35 m.

3. 2. *Western Antarctic Peninsula (WAP)*

The WAP measurements used for the model inputs were taken from the midsummer (January) cruise in 1996 in the Palmer LTER regional sampling grid (Figure 3) and from inshore sites near Palmer Station, also during January. All of the WAP data were obtained from the Palmer LTER website (http://pal. lternet. edu/datausepolicy_03pal. html), unless otherwise noted. January is a critical time for Adélie penguin chick development and is coincident with the crèche period, when both parents leave the chicks on land and forage, doubling the food provided to the chicks (Salihoglu et al., 2001). Data for the models were taken from stations within the foraging area of the Adélie penguins (Figure 3). The sampling area is defined by the seaward part of a circular area centered on Anvers Island, the home of the local Adélie colony, and with a radius equal to the foraging distance of the adult Adélies: 113 km for January, 1996 (Culik and Wilson, 1991; W. Fraser, unpublished data). The 1999 foraging area is also shown for comparison. The krill biomass was much less in 1999 and the penguins had to forage over a larger area (Daniels 2003).

The measurements were averaged over January to provide values to use in the model (Table 1). All data were integrated to a depth of 35 m, unless otherwise stated, to allow for direct comparison with the NABE results. The measurements for the western Antarctic Peninsula were not a time series, as in NABE, but were taken from selected stations on the regional and local

sampling grids. Given the sampling scheme, it was not possible to estimate changes in the biomasses of food web components over the study period. It was assumed that biomass did not change over the month and the balance equations for each component were set to zero. An analysis of an inverse method applied to data sampled from a simulated plankton food web in a transient state and assuming no change in the mass balance components was shown to be just as accurate as the method applied to the same food web in steady state (Vézina and Pahlow, 2003).

Primary production (Figure 4) was measured to the 2% light level, which was almost always above 35 m, so the integrated production was representative of the entire euphotic zone. 2/3 of the measured primary production was assigned to the large phytoplankton (> 5 μm) and 1/3 to the small (< 5μm). The phytoplankton community in the Palmer region is dominated by larger cells (diatoms) during bloom conditions (Garibotti, 2003). Chlorophyll *a* was measured by fluorometry and converted to carbon biomass (Figure 4) using a C:Chl ratio of 50 (Holm-Hansen and Mitchell, 1991). Bacterial production in the WAP was estimated by the inverse routine because measured production was not available in carbon units. The bacterial production was constrained to be within a broad range of zero and fifty percent of the primary production so as not to force the solution to a particular value. Bacterial biomass (Figure 4) was determined from measurements of particulate lipopolysaccharide. Microzooplankton grazing was not measured as part of the Palmer LTER study. Estimates from different areas of the Southern Ocean including the Ross Sea (Caron et al., 2000), and the Atlantic sector (Becquevort, 1995; Froneman, 1996) were used to provide a wide range of potential microzooplankton grazing from 0 – 75% of primary production. Microzooplankton biomass was not measured, so the upper bound of microzooplankton respiration was left unconstrained.

Antarctic krill (*Euphasia superba*) biomass was estimated from penguin stomach content data, trawl data, and other estimates from the literature. Penguins are opportunistic visual predators that do not discriminate between different sizes of krill, so the size distribution of krill in their stomachs is a good approximation of the size distribution of krill in the area (Salihoglu et al., 2001). The average krill sizes were used to estimate the individual wet weight of an average krill, using regressions established by R. Ross and L. Quetin (unpublished data) between length and wet weight of krill measured in trawl catches. The density of krill measured in trawls was then used to find the biomass of krill. The biomass of krill was also estimated from acoustic data taken with an echo sounder within the regional grid (Lascara et al., 1999). Krill grazing (Table 1) was estimated from a feeding relationship established in experiments during 1991 and 1992 by Ross et al. (1998). The average phytoplankton concentration in the upper 35 m was used in the feeding relationship to estimate the mass specific feeding rate. The trawl and acoustic biomass measurements were used to find minimum and maximum population grazing estimates, respectively.

Export of particulate carbon was measured at a sediment trap located near Palmer Station at a depth of 150 m (Table 1). The export at 35 m was estimated using the measurements at 150 m and assuming a normalized power function derived for open ocean environments (Martin et al., 1987): $F = F_{100} (z/100)^{b}$. The known export at 150 m was used to estimate F_{100} using the above equation and assuming b = - 0. 858 (Martin et al., 1987). The export at 35 m was then estimated using the above equation. There can be a large uncertainty in extrapolating the exponential power function over a large depth range, so we used the extrapolated value ± 50% as a target for the solutions.

4. Results.

4. 1. North Atlantic Bloom Experiment Inverse Model Results

The bacterial carbon demand and grazing by microzooplankton and protozoans dominated the flows of carbon in the North Atlantic inverse solution (Figure 1a and Table 2). Bacterial carbon demand was the largest flow (46.7 mmol C m^{-2} d^{-1}) equal to 74% of the net primary production. The microzooplankton and protozoans together dominated grazing. Microzooplankton grazing of small and large phytoplankton carbon removed 44% of the NPP while protozoans grazed 21% of the NPP as small phytoplankton. Mesozooplankton grazing of large phytoplankton was equal to just 6% of the NPP. The export or e-ratio for NABE was derived by summing the sinking detritus and the mesozooplankton export (transfer of mesozooplankton to higher trophic levels not modeled or mortality) and normalizing to the primary production: 0.12 + 0.01 = 0.13 (Table 2).

4. 2. Western Antarctic Peninsula Inverse Model Results

The largest flows within the food web inferred from the WAP model solution were krill grazing and respiration, equivalent to 40 and 21% of the NPP, respectively (Figure 1b and Table 2). The next most important flows were microzooplankton respiration (20% of NPP), protozoan respiration (16% of NPP) and bacterial carbon demand (15% of NPP), which channeled a significant amount of carbon into the microbial food web. Thus while short food web (diatom-krill) processes were the dominant flows, microbial food web processes were important as well. The particulate carbon export from the top 35 m was equal to 8.7 mmol C m^{-2} d^{-1} or 9% of the primary production (Table 2). The export of krill, representing krill production that can be consumed by higher trophic levels or else sink when the krill die, was an additional 18% of the

primary production. The estimated export (e-) ratio was equal to the sum of the particulate export and the krill export normalized to the primary production: 0.09 + 0.18 = 0.27.

4. 3. North Atlantic vs. Western Antarctic Peninsula

A direct comparison was made between the WAP and NABE carbon models in order to investigate differences in the trophic functioning expressed in the two regions, as a result of the different food web structures. This comparison is meaningful because the inferred primary production in the regions was similar: 66 mmol C m^{-2} d^{-1} for NABE and 94 mmol C m^{-2} d^{-1} for the WAP carbon model (large and small phytoplankton gross primary production minus the large and small phytoplankton respiration from Table 2).

The largest flow within the WAP food web was the krill grazing of large phytoplankton, while the largest flow within the NABE food web was bacterial carbon demand (Table 2 and Figure 1). The sum of microzooplankton and protozoan grazing in the NABE model was almost twice as great as in the WAP model relative to primary production (Table 2). NPP-normalized krill grazing in the WAP model was almost 7 times larger than mesozooplankton grazing in the NABE model. The estimated e-ratio for the WAP of 27% was about twice as high as the NABE e-ratio of 13%, even though the particulate export in the NABE model was slightly higher. Food web transfer to higher trophic levels made a large contribution to the WAP e-ratio.

4. 4. Comparison of short food web vs. microbial food web

The short diatom-krill-predator food chain is believed to be the most significant pathway for carbon in coastal waters of the Southern Ocean (Huntley et al., 1991). In contrast the microbial food web is now believed to play an active role in the North Atlantic bloom (Ducklow et al., 1993; Harrison et al., 1993; Lochte et al., 1993). The relative activities of the short or

classical food chain and microbial food webs are given in Table 3. All of the flows within the short food web that lead to export out of the surface ocean through sinking or transfer to higher trophic levels were summed. The flows within the microbial food web were also summed, including all flows between the microbial organisms and their interactions with the detritus and DOC pools. The ratio of microbial to short food web flows was 1.2 for the WAP solution, suggesting equal activity by each assemblage. In NABE, the microbial food web was 9 times more active than the short food web.

In the NABE model, detritus, microzooplankton and protozoans made the largest contributions to the DOC pool (Figure 5a). In the WAP model, krill and large phytoplankton were the biggest contributors to the DOC pool and sizable inputs were received from all the living components (Figure 5b). Particle decay from detritus contributed 55% of the DOC pool in the NABE solution, but did not contribute to the DOC pool in the WAP solution.

4. 5. Comparison of network analysis indices

Network analysis indices were used to further explore the relative activity of each living and nonliving compartment. A comparison of these trophic indices for the 2 models indicates that bacterial production was much greater in NABE, where it accounted for 26% (***Fbac*** = 26%) of the primary production vs. 1% (***Fbac*** = 1%) in the WAP model (Table 4). The dominance of krill in the WAP was evident with the krill processing 49% (***Fkri*** = 49%) of the total carbon passing through all the grazers (Table 4). The dominance of microzooplankton and protozoans in the North Atlantic was obvious with the total throughput of microzooplankton and protozoans equal to 90% (***Fmic*** = 49%, ***Fpro*** = 41%) of the total carbon passing through all the grazers (Table 4). For the North Atlantic model, 108% of the primary production passed through the

DOC pool while in the WAP model, just 15% of the primary production cycled as DOC. The detritus pool received 25% of the primary production in the WAP model, while in the NABE model it received 77% .

The recycling index, **L** and the **Total Ingestion / PP** indicated greater recycling in the North Atlantic than the western Antarctic Peninsula. The average carbon atom cycles within the North Atlantic food web 3 times before exiting through respiration or sinking, while **L** for the western Antarctic Peninsula is 1.5 (Table 4). The **Total Ingestion / PP** indicates that in the North Atlantic food web, zooplankton and bacteria process 160% of the primary production, indicating a strong reliance on recycled carbon (Table 4). In the western Antarctic Peninsula food web, the zooplankton and bacteria process 115% of the primary production, indicating somewhat less reliance on recycled carbon.

The effective trophic levels found using the NETWRK program (Ulanowicz, 1986) showed a simpler food web for the WAP than for NABE (Table 5). The large and small phytoplankton, detritus, and DOC compartments are all arbitrarily assigned trophic levels of 1. In the WAP, the protozoans, microzooplankton, and krill all fed at trophic levels close to 2 (Table 5). In the NABE solution, a more complex picture was evident, with the grazers feeding at trophic levels farther from 2.

Overall, these analyses of the flow network solutions suggest a microbe-dominated bloom in the North Atlantic with high reliance on recycling and active detrital pools (particulate and dissolved), while the opposite tended to be the case for the WAP. The Antarctic system was dominated by larger organisms, with lower activity in the microbes and detritus pools, and less dependence on recycling.

4. 6. Sensitivity Analysis

The input parameters to the NABE carbon model were successively varied by ±10% and the inverse solution was recalculated for each change to assess the sensitivity of the model to these variations (Figure 6). All 35 flows were invariant to changes in four of the eleven inputs. Three of the eleven inputs brought about changes of greater than 10% in 6 or fewer flows. The four inputs that had the greatest effects on the flows are discussed here. The +/- 10% changes in the large and small phytoplankton had the largest effects, bringing about changes of greater than 10% in 18 of the 35 flows (Figure 6a). 6 these flows changed by more than 40%. The +/- 10% changes in the microzooplankton feeding affected 11 of the 35 flows and changes in the bacterial production affected 9 flows (Figure 6b). All these inputs were well-constrained by observation. The flows that were sensitive to the greatest number of input parameters, also each represented less than 2% of the net primary production; large phytoplankton release of DOC (sensitive to 6 of the 11 the input parameters), small phytoplankton release of DOC (sensitive to 6 input parameters), and mesozooplankton consumption of microzooplankton (sensitive to 7 input parameters).

In the WAP model, all 35 flows were invariant to 7/12 of the input parameters that were decreased by 10% and 8/12 of the parameters that were increased by 10%. Changes in the large and small net primary production also had the greatest effects on the flows, as in the NABE model, with ±10% changes in 25 of the 35 food web flows (Figure 7a). These inputs were also well constrained by observation. Ten of these flows were affected by more than 40% with the decrease in large phytoplankton production by 10% but only one flow was changed by more than 40% with the increase. Changes in the bacterial production had the next greatest effect on the

flows, as seen in the NABE model. The increase of 10% in the minimum bacterial production brought about changes of greater than 10% in 12 of the flows (Figure 7b) but the decrease did not bring about any change in the flows. The changes in the krill minimum grazing brought about changes greater than 10% in 8 of the flows. The export for the WAP model was varied by +/- 50% to reflect the uncertainty of the exponents used in the Martin flux to depth relationship. Seven of the flows changed by more than 10% but none changed by more than 40%, except for the detritus to export flow itself that increased 50% with the increase and decreased 50% with the decrease.

5. Discussion

5.1. Accuracy of the model results.

Inverse model results represent extrapolations of food web structure from a small set of measured flows and a larger set of constraints and mass balance considerations. There is a large (potentially infinite) number of solutions consistent with the observations and constraints, and the question arises as to the accuracy and realism of the model solutions. Some criterion is needed to select the best solution. The standard criterion in almost all geophysical and ecological inversions is the solution that minimizes the sum of the squares of the estimated components (the food web exchanges or flows in ecological applications). As discussed at length in Vézina and Pahlow (2003), for ecosystem inversions this amounts to evening out the flows in a system, tending to increase small flows and decrease larger ones. It is not possible to assess empirically the accuracy of an inverse solution without a reliable and comprehensive set of measurements of flows. Vézina and Pahlow (2003) addressed this problem by subsampling flow data from a

numerical simulation model of a generic plankton system, and using these subsets as "observations" to obtain inverse solutions, then comparing the estimated flows to the original simulation results. They found that the inverse method provided substantially accurate representations of the original data under a wide variety of conditions.

Vézina and Pahlow (2003) tested their inverse methodology by sampling from steady-state simulations representing winter, spring and summer conditions, and from three stages of a transient simulation similar to a phytoplankton bloom. Although reasonably accurate representations of the original systems were obtained under all conditions, the inverse results proved to be less accurate as systems evolved from winter toward summer. Winter-spring conditions, characterized by less recycling and higher export were more accurately reproduced than summer conditions with greater recycling, less export (lower e-ratios) and more complex food webs. Transient states produced more accurate results than the steady-state cases. In most cases, the inverse solutions tended to overestimate flows of smaller magnitude and underestimate larger flows. Their findings have several implications for our study.

First, phytoplankton blooms are emblematic of non-steady state plankton systems. Inverse solutions have tended to assume steady state due to the frequent use of snapshots of data. Vézina and Pahlow's (2003) results imply that inverse solutions for phytoplankton blooms are not *a priori* likely to be in great error, just because they are not near a steady state. Second, their finding that inverse approaches worked better on winter-spring systems with lower recycling implies that the NABE and WAP systems are good cases for application of this methodology. It is true that the NABE data implied a bloom system with larger than expected recycling; and to the extent this was so, the inverse solution may be less accurate than the WAP case, with low

recycling. Finally, Vézina and Pahlow (2003) suggested that inverse solutions tended to even out flows in the recovered solutions. Our solutions for both NABE and WAP exhibited flows with a wide range of magnitudes. That is, both systems were characterized by very large and very small flows (e.g., krill grazing and bacterial production in the WAP; and bacterial production and mesozooplankton grazing in NABE). If the inverse method behaved in our solutions as it did for Vézina and Pahlow (2003), our modeled flows appear to be robust representations of the real systems.

The findings of Vezina and Pahlow (2003) bear on our results to the extent that the food web model they tested, and that the "observations" they used in inverse reconstructions were similar to ours. Vezina and Pahlow (2003) used a food web with 2 size classes of phytoplankton and zooplankton, bacteria, DOC and detritus, very similar to our food web with large and small phytoplankton and 3 grazers. Their input observations included just the primary production, export flux and bacterial production, leaving all the grazer and metabolic (respiration and decay) terms to be estimated by the inverse model. Thus their input data and ours were similar and similarly sparse. We believe that their results likely reflect similar performance by our model.

5. 2. Comparison of NABE and WAP Food Webs

Krill were the dominant organisms affecting the flow of carbon in the WAP food web and microbial organisms were dominant in the North Atlantic. The greatest flows within the WAP model were related to krill, while the greatest flows within the NABE model were bacterial carbon demand and microzooplankton grazing. The dominance of krill is not surprising given that they usually dominate the zooplankton biomass in the WAP (Ross et al. 1998). In 1996 krill biomass was 227 mmol C m^{-2} (Table 1) vs. the mesozooplankton biomass of 7 mmol C m^{-2}

(Table 1) in the North Atlantic in May 1989. The krill biomass was equal to almost 1/3 of the phytoplankton biomass in the WAP.

Active recycling was evident in the North Atlantic model, while only weak recycling was seen in the western Antarctic Peninsula model. In the NABE model, the microbial food web flows processed about 9 times more carbon than the short food web. In the WAP model, the short food web and microbial food web flows processed equal amounts of carbon, even though the short food web has traditionally been thought to be dominant in the Southern Ocean and other marginal ice zone systems (Huntley et al. 1991).

Bacterial production was much greater in the NABE food web. In the WAP model, bacterial production was just 1% of the NPP (Table 4). The bacterial uptake of DOC was about 5 times greater in the NABE model, 74% of primary production vs. 15% for the WAP. Similar results to NABE were found farther north in the Greenland Sea, where the accumulation of DOC in the surface waters was estimated to be greater than 50% of the new production (Noji et al. 1999). The build-up of DOC in the Greenland Sea is also believed to drive high bacterial production. The results for the WAP agree in part with earlier observations of low bacterial production during the spring bloom in the Gerlache strait, just north of the Palmer area (Karl et al. 1999b). High grazing rates on bacteria were measured in dilution experiments in areas of high phytoplankton biomass during the bloom (Karl et al. 1999b). The WAP model showed very low grazing of bacteria, equal to just 1% of the primary production but equal to 100% of the bacterial production. Despite low bacterial production, the bacteria still played a relatively active role in the food web by ingesting 14% of the primary production as DOC and respiring most of this uptake (13%). Large ranges were assigned to the constraints for bacterial production and

microzooplankton grazing in the WAP, because these processes are highly variable across the world's oceans and not well documented in the Southern Ocean (Caron et al., 2000; Froneman and Perissinotto, 1996; Becquevort, 1995; Karl, 1996). The microzooplankton grazing inferred by the inverse method was 21% of the primary production in 1996 and 26% in 1999 (results in Daniels 20003).

The estimated e-ratio of 0.27 for the WAP model was higher than in the NABE model (e = 0.13), with krill export production equaling 19% of the WAP primary production. In the WAP full carbon model (Daniels 2003), penguins and myctophids together consumed just 1% of the primary production in the form of krill. This left 18% of the primary production that could go to an increase in krill biomass or be passed up the food web to other (unmodeled) predators. Baleen whales consume an estimated 10% of krill production in the Southern Ocean (Laws, 1985) and could consume some of this krill production. Krill biomass is highly variable across seasons with up to an order of magnitude increase from fall/winter to spring /summer (Lascara et al., 1999), so a significant increase in krill biomass is also possible.

The NABE model apportioned the new production differently than was implied by floating sediment trap data. The modeled e-ratio of 0.13 for NABE was about half the value of 0.45 estimated by Martin et al. (1993) from floating sediment traps. We used ^{234}Thorium data to constrain the particle export in NABE, which tended to provide lower estimates than the traps (Buesseler et al., 1992). The model is more consistent with the conclusions of Garside and Garside (1993), who suggested that not all the new production was exported, but remained in the food web during the observation period. Our solution accounted for a sink for this unrealized export with the inclusion of the observed increases in biomass of bacteria and microzooplankton

(Table 1).

Other food web flows that were inferred by the inverse method not otherwise measured include interactions with the detrital pools. In both models, the total throughput in the detritus pool was a substantial portion of the primary production. In an inverse analysis of a plankton food web off Southern California, Jackson and Eldridge (1992) also found detritus was an active component, receiving large contributions from sinking phytoplankton and making significant contributions to the dissolved organic matter pool. In the NABE carbon solution, the dissolution of detritus made up 55% of the input to the DOC pool. In an inverse analysis of a plankton food web of the Takapoto Atoll in French Polynesia, Niquil et al. (1998) suggested that detritus played an important role providing food for all of the zooplankton components. In the WAP carbon solution, all of the zooplankton classes consumed detritus with the protozoans consuming 7% of the net primary production (Table2). However, in the NABE solution there was no consumption of detritus by the zooplankton.

The sensitivity analysis results reaffirmed the model results for NABE and the WAP. Changes in the phytoplankton production had the greatest effects on the flows for both models. This is not surprising, given that the phytoplankton production is the input that drives the food webs and also represents the greatest flows in the models. For NABE, microzooplankton grazing and bacterial production also affected the flows significantly. The microzooplankton and bacteria were very active in the NABE solution representing the greatest consumption of carbon by organisms within the model. In the WAP sensitivity analysis, bacterial production and krill grazing had significant effects on the flows. Bacteria were active in the WAP solution, taking up 14% of the primary production and krill were the most active living component.

5. 3. Classification of Food Webs

Once the complete pattern of flows in a system is determined, it can be classified according to various schemes. Legendre and Rassoulzadegan (1996) described three pathways for carbon flow through a food web: the sinking of ungrazed phytoplankton, food web transfer, and recycling. They related these three food web processes to the size structure of the phytoplankton and matching (synchronization) of phytoplankton production with grazing. Legendre and Rassoulzadegan derived analytical solutions for the proportion of the primary production allocated to each of the three pathways based on the ratio of large phytoplankton production to total phytoplankton production, $\mathbf{P_L/P_T}$, and the matching between phytoplankton production and grazing, **M**. They used values from the literature to estimate the magnitude of these food web functions for 5 different types of food webs (Table 6). The food web types ranged along a continuum of decreasing ratios of export to primary production. At one extreme is the sinking of ungrazed phytoplankton, representing a food web with high primary production that is not matched by grazing. At the other extreme is the microbial loop, an almost closed system with near zero input of primary production, consisting of bacteria and protozoans. In between the two extremes in order of decreasing export/ production are the herbivorous, multivorous, and microbial food webs. Legendre and Rassoulzadegan (1996) found good agreement between their derived values of food web function and the estimates from the literature, supporting their assumption that the size structure of the phytoplankton and degree of matching strongly determined food web structure.

The 3 food web functions for five different types of food webs provide a baseline to compare estimates of these functions from the WAP and NABE carbon models (Table 6). The

food web transfer described by Legendre and Rassoulzadegan (1996), $\mathbf{F_T/P_T}$, includes any carbon passed up the food chain that is exported out of the surface ocean by sinking or transfer to higher trophic levels. This includes the fecal pellets and export production of mesozooplankton or krill. $\mathbf{D_T/P_T}$ is the fraction of ungrazed, sinking phytoplankton. In our models, $\mathbf{D_T/P_T}$ can be equated with the large phytoplankton to detritus flows. However, unlike the Legendre model, our models also include a particulate detritus pool where the large phytoplankton collect before sinking. In both of our solutions the large phytoplankton to detritus flows were greater than the detritus to export flows, reflecting recycling of large phytoplankton detritus. Therefore, to be conservative we used the detritus to export flows for $\mathbf{D_T/P_T}$. The recycling pathway, $\mathbf{R_T/P_T}$ was found by subtracting the total export equal to the sum of $\mathbf{F_T/P_T}$ and $\mathbf{D_T/P_T}$, from the total net primary production, equal to 1.0.

The NABE model has food web functions lying between the microbial food web and the microbial loop categories even though the segregation of the primary production $\mathbf{P_L/P_T}$ of 0.5 is much higher than assumed for these systems. The recycling pathway consumes a high proportion of the primary production, $\mathbf{R_T/P_T}$ = 0. 84, putting the North Atlantic food web between the microbial food web and the microbial loop. The food web transfer, $\mathbf{F_T/P_T}$ of 0.04 is very low, putting the food web close to the microbial loop, while the sinking phytoplankton pathway, $\mathbf{D_T/P_T}$ of 0.12 is close to the multivorous food web value (0.1) but not far from the microbial loop and food web values (each equal to 0).

The WAP solution lies between the multivorous food web and the microbial food web categories. The recycling pathway, $\mathbf{R_T/P_T}$ of 0.69 is between the multivorous and microbial food web. The food web transfer pathway, $\mathbf{F_T/P_T}$ of 0.22 is very close to that of the microbial food

web and the sinking pathway $\mathbf{D_T/P_T}$ 0.09 is very close to the multivorous food web value.

The inverse solutions give values of the food web functions that are somewhat different than would be expected using Legendre and Rassoulzadegan's (1996) assumptions about the size distribution of primary production. The size distribution of primary production for each of the inverse models indicate food webs lying somewhere between the multivorous and herbivorous food webs. However, the food web functions calculated from the inverse model results put the North Atlantic food web somewhere between the microbial food web and microbial loop and the western Antarctic Peninsula food web between the multivorous and microbial food webs. The matching parameter used by Legendre and Rassoulzadegan is an arbitrary parameter that is not related directly to measurements. For NABE, the matching between grazers and phytoplankton was likely high because the fast growing microzooplankton and protozoans dominated the grazing and there was no increase in phytoplankton during the study. This high degree of matching would push the NABE food web towards higher recycling in the direction of the microbial loop. For the WAP, the dominance of krill grazing would give a lower degree of matching than in NABE because of the relatively slower growth of krill to microzooplankton and push the food web towards the extreme of sinking of ungrazed cells. These findings appear to reveal a bias in both of the inverse solutions towards the microbial loop extreme. The assumptions from Legendre and Rassoulzadegan are based on only a few food webs, so it is possible that with data from more systems these descriptions of food web types would be different and biased towards higher recycling. It is also possible that model solutions like ours, where all flows are known, give different results than observed systems for which our knowledge remains incomplete.

Acknowledgements.

We are grateful to George Jackson for providing his software and much guidance during this project. Bill Fraser, Robin Ross and Langdon Quetin provided data and answered questions about the WAP system. This research was supported by US JGOFS Synthesis and Modeling Project NSF grants, OCE-0097237 to HWD and OCE-0097296 to G. Jackson (TAMU) and by NSF/ONR 00014210370 (NOPP) awarded to L. Rothstein (URI) as subcontracted to HWD. WAP data synthesis supported by NSF OPP 0217282. This is US JGOFS Contribution YYYY.

References Cited

Baines, S.B., Pace, M.L., 1991. The production of dissolved organic matter by phytoplankton and its importance to bacteria: patterns across marine and freshwater systems. Limnology and Oceanography 36, 1078-1090.

Becquevort, S., 1995. Nanoprotozooplankton in the Atlantic sector of the Southern Ocean during early spring: biomass and feeding activities. Deep Sea Research II 44, 355-373.

Buessler, K.O., Bacon, M.P., Cochran, J.K., Livingston, H.D., 1992. Carbon and nitrogen export during the JGOFS North Atlantic bloom experiment estimated from 234Th: 238U disequilibria. Deep Sea Research II 39, 1115-1137.

Capriulo, G.M., 1990. Feeding-Related Ecology of Marine Protozoa. In: Capriulo, G.M. (Ed.), Ecology of Marine Protozoa. Oxford University Press, New York, NY, pp 186 1990.

Carlson, C.A., Ducklow, H.W., Michaels, A.F., 1994. Annual flux of dissolved organic carbon from the euphotic zone in the northwestern Sargasso Sea. Nature 371, 405-408.

Caron, D.A., Dennett, M.R., Lonsdale, D.J., Moran, D.M., Shalapyonok, L., 2000. Microzooplankton herbivory in the Ross Sea, Antarctica. Deep Sea Research II 47, 3249-3272.

Culik, B.M., Wilson, R.P., 1991. Energetics of underwater swimming in Adélie penguins. Journal of Comparative Physiology 161, 285-291.

Dam, H.G., Miller, C.A., Jonasdottir, S.H., 1993. The trophic role of mesozooplankton at 47°N, 20°W during the North Atlantic Bloom Experiment. Deep Sea Research II 40, 197-212.

Dam, H.G., Zhang, X., Butler, M., Roman, M.R., 1995. Mesozooplankton grazing and metabolism at the equator in the central Pacific: Implications for carbon and nitrogen fluxes. Deep Sea Research 42, 735-756.

Daniels, R.M., 2003. Inverse model analysis of plankton food webs in the north Atlantic and western Antarctic Peninsula. Master's Thesis, College of William and Mary, Virginia Institute of Marine Science, Gloucester Point, VA. 1-178.

Donali, E., Olli, K., Heiskanen, A.S., Andersen, T., 1998. Carbon flow patterns in the planktonic food web of the Gulf of Riga, the Baltic Sea: a reconstruction by the inverse method. Journal of Marine Systems 23, 251-268.

Ducklow, H.W., 2003. Chapter 1. Biogeochemical Provinces: Towards a JGOFS Synthesis. In: Fasham, M.J.R., (Ed.), Ocean Biogeochemistry: A New Paradigm. Springer-Verlag, New York, pp. 3-18.

Ducklow, H.W., Fasham, M.J.R., Vezina, A.F., 1989. Derivation and analysis of flow networks for oceanic plankton systems. In: Wulff, F., Field, J.G., Mann, K.H. (Eds.), Network Analysis in Marine Ecology. Springer-Verlag, Berlin, pp. 159-205.

Ducklow, H.W., Harris, R., 1993. Introduction to the JGOFS North Atlantic bloom study. Deep-Sea Research II 40, 1-8.

Ducklow, H.W., Kirchman, D.L., Quinby, H.L., Carlson, C.A., Dam, H.G., 1993. Stocks and dynamics of bacterioplankton carbon during the spring phytoplankton bloom in the eastern North Atlantic Ocean. Deep-Sea Research II 40, 245-63.

Dugdale, R.C., Goering, J.J., 1967. Uptake of new and regenerated forms of nitrogen in primary production. Limnology and Oceanography 12, 196-206.

Eldridge, P.M., Jackson, G.A., 1993. Benthic trophic dynamics in California coastal basin and continental slope communities inferred using inverse analysis. Marine Ecology Progress Series 99, 115-135.

Eppley, R.W., Peterson, B.J., 1979. Particulate organic matter flux and planktonic new production in the deep ocean. Nature 282, 677-680.

Fasham, M.J.R., 1995. Variations in the seasonal cycle of biological production in subarctic oceans: A model sensitivity analysis. Deep-Sea Research 42, 1111-1149.

Fuhrman, J.A., Sleeter, T., Carlson, C.A., Proctor, L.M., 1989. Dominance of bacterial biomass in the Sargasso Sea and its ecological implications. Marine Ecology Progress Series 57, 207-217.

Froneman, P., and R. Perissinotto, 1996. Microzooplankton grazing in the Southern Ocean: implications for the carbon cycle. P.S.Z.N.I.: Marine Ecology 17, 99-115.

Garibotti, I.A., Vernet, M., Ferrario, M.E., Smith, R..C., Ross, R.M., Quetin, L.B., 2003. Phytoplankton spatial distribution in the Western Antarctic Peninsula (Southern Ocean). Marine Ecology Progress Series 261, 21-39.

Garrison, D.L., Gowing, M.M., Hughes, M.P., Campbell, L., Caron, D.A., Dennett, M.R., Shalapyonok, L., Olson, R.J., Landry, M.L., Brown, S.L., Liu, H.-B., Azam, F., Steward, G., Ducklow, H.W., Smith, D.C., 2000. Microbial food web structure in the Arabian Sea: A U. S. JGOFS Study. Deep-Sea Research II 47, 1387-1422.

Garside, C., Garside, J., 1993. The "f-ratio" on 20W during the North Atlantic Bloom Experiment. Deep-Sea Research II 40, 75-90.

Harrison, W.G., Head, E.J.H., Horne, E.P.W., Irwin, B., Li, W.K.W., Longhurst, A.R., Paranjape, M.A., Platt, T., 1993. The western North Atlantic bloom experiment. Deep-Sea Research II 40, 279-305.

Holm-Hansen, O., Mitchell, B.G., 1991. Spatial and temporal distribution of phytoplankton and primary production in the western Bransfield Strait region. Deep-Sea Research 38, 961-980.

Huntley, M.E., Lopez, M.D.G., Karl, D.M., 1991. Top predators in the Southern Ocean: A Major Leak in the Biological Carbon Pump. Science 253, 64-66.

Jackson, G., and P.M. Eldridge, 1992. Food web analysis of a planktonic system off Southern California. Progress in Oceanography 30, 223-251.

Joint, I., Pomroy, A., Savidge, G., Boyd, P., 1993. Size-fractionated primary productivity in the northeast Atlantic in May-July 1989. Deep Sea Research II 40(1/2), 423-440.

Karl, D.M., 1999a. A sea of change: Biogeochemical variability in the North Pacific

subtropical gyre. Ecosystems 2, 181-214.

Karl, D.M., 1999b. Uncoupling of bacteria and phytoplankton during the austral spring bloom in Gerlache Strait, Antarctic Peninsula. Aquatic Microbial Ecology 19, 13-27.

Karl, D.M., Christian, J.R., Dore, J.E., Letelier, R.M., 1996. Microbiological oceanography in the region west of the Antarctic Peninsula: Microbial dynamics, nitrogen cycle and carbon flux. In: Ross, R.M., Hofmann, E.E., Quetin, L.B. (Ed.s), Foundations for ecological research west of the Antarctic Peninsula. American Geophysical Union, Washington, DC, pp. 303-332.

Kato, S., 1982. Taxomic studies on the genus Euglena in Japan. Journal of Japanese Botany 57, 217-222.

Lancraft, T.M., Hopkins, T.L., Torres, J.J., Donnelly, J., 1991. Oceanic micronektonic/macrozooplanktonic community structure and feeding in the ice covered Antarctic water during the winter (AMERIEZ 1988). Polar Biology 11, 157-167.

Landry, M.R., Barber, R.T., Bidigare, R.R., Chai, F., Coale, K.H., Dam, H.G., Lewis, M.R., Lindley, S.T., McCarthy, J.J., Roman, M.R., Stoecker, D.K., Verity, P.G., White, J.R., 1997. Iron and grazing constraints on primary production in the central equatorial Pacific: an EqPac synthesis. Limnology and Oceanography 42, 405-418.

Lascara, C.M., Hofmann, E.E., Ross, R.M., Quetin, L.B., 1999. Seasonal variability in the distribution of Antarctic krill, *Euphausia superba*, west of the Antarctic Peninsula. Deep-Sea Research I 46 , 951-984.

Laws, R.M., 1985. The Ecology of the Southern Ocean. American Scientist 73, 26-40.

Legendre, L., Gosselin, M., 1989. New production and export of organic matter to the deep ocean: consequences of some recent discoveries. Limnology and Oceanography 34, 1374-1380.

Legendre, L., Rassoulzadegan, F., 1996. Food-web mediated export of biogenic carbon in oceans: hydrodynamic control. Marine Ecology Progress Series 145, 179-193.

Lochte, K., Ducklow, H.W., Fasham, M.J.R., Stienen, C., 1993. Plankton succession and carbon cycling at 47º N 20º W during the JGOFS North Atlantic Bloom Experiment. Deep-Sea Research II 40, 91-114.

Longhurst, A.R., 1995. Seasonal cycles of pelagic production and consumption. Progress in Oceanography 36, 77-167.

Longhurst, A.R., 1998. Ecological Geography of the Sea. Academic Press, San Diego, pp 1-398.

Martin, J.H., Fitzwater, S.E., Gordon, R.M., Hunter, C.N., Tanner, S.J., 1993. Iron, primary production and carbon-nitrogen flux studies during the JGOFS North Atlantic Bloom Experiment. Deep-Sea Research II 40, 115-134.

Martin, J.H., Knauer, G.A., Karl, D.M., Broenkow, W.W., 1987. VERTEX: Carbon cycling in the Northeast Pacific. Deep-Sea Research 34, 267-285.

Michaels, A.F., Silver, M.W., 1988. Primary production, sinking fluxes and the microbial food

web. Deep-Sea Research 35, 473-490.

McCarthy, J.J., Garside, C., Nevins, J.L., Barber, R.T., 1996. New production along 140º W in the Equatorial Pacific during and following the 1992 El Nino event. Deep-Sea Research II 43, 1065-1093.

Moloney, C.L., Field, J. G., 1989. General allometric equations for rates of nutrient uptake, ingestion, and respiration in plankton organisms. Limnology and Oceanography 34, 1290-1299.

Niquil, N., Jackson, J.B.C., Legendre, L., Dellesalle, B., 1998. Inverse model analysis of the planktonic food web of Takapoto Atoll (French Polynesia). Marine Ecology Progress Series 165, 17-29.

Noji, T.T., Rey, F., Miller, L.A., Borsheim, K.Y., Urban-Rich, J., 1999. Fate of biogenic carbon in the upper 200 m of the central Greenland Sea. Deep-Sea Research II 46, 1497-1509.

Pakhomov, E.A., Perissinotto, R., McQuaid, C.D., 1996. Prey composition and daily rations of myctophid fishes in the Southern Ocean. Marine Ecology Progress Series 134, 1-14.

Parker, R.L., 1977. Understanding inverse theory. Annual Review of Earth Planetary Science 5, 35-64.

Pauly, D., Christensen, V., Walters, C., 2000. Ecopath, Ecosim, and Ecospace as tools for evaluating ecosystem impact of fisheries. ICES Journal of Marine Science 57, 697-706.

Perissinotto, R., A. Pakhomov, E., 1998. The trophic role of the tunicate *Salpa thompsoni* in the Antarctic marine ecosystem. Journal of Marine Systems 17, 361-374.

Pesant, S., Legendre, L., Gosselin, M., Ashjian, C., Booth, B., Daly, K., Fortier, L., Hirche, H.J., Michaud, J., Smith, R.E.H., Smith, S., Smith, W.O., Jr., 1998. Pathways of carbon cycling in the euphotic zone: the fate of large-sized phytoplankton in the Northeast Water Polynya. Journal of Plankton Research 20, 1267-1291.

Pomeroy, L.R., 2001. Caught in the food web: complexity made simple? Scientia Marina 65 (Suppl. 2), 31-40.

Repeta, D. "North Atlantic Bloom Experiment HPLC pigments from Atlantis II cruise 119 leg 5." United States JGOFS Process Study Data 1989-1998; CD-ROM volume 1, version 2, Woods Hole Oceanographic Institution, USA: U.S. JGOFS Data Management Office, April 2003.

Richardson, T.L., Jackson, G.A., Ducklow, H.W., Roman, M.R. 2004. Carbon fluxes through food webs of the eastern equatorial Pacific: an inverse approach. Deep-Sea Research I 51, 1245-1274.

Richardson, T.L., Jackson, G.A., Ducklow, H.W., Roman, M.R. 2005. Spatial and seasonal patterns of carbon cycling through planktonic food webs of the Arabian Sea determined by inverse analysis. Deep-Sea Research II XX, yyyy-yyyy. (this volume).

Rivkin, R.B., Legendre, L., Deibel, D., Tremblay, J.E., Klein, B., Crocker, K., Roy, S., Silverberg, N., Lovejoy, C., Mesplé, F., Romero, N., Anderson, M.R., Matthews, P., Savenkoff, C., Vézina, A., Therriault, J.C., Wesson, J., Bérubé, C., Ingram, R.G., 1996.

Vertical flux of biogenic carbon in the ocean: is there food web control? Science 272, 1163-1166.

Ross, R.M., Quetin, L.B., Lascara, C.M., 1996. Distribution of Antarctic krill and dominant zooplankton west of the Antarctic Peninsula. In: Ross, R.M., Hofmann, E.E., Quetin, L.B. (Eds.), Foundations for Ecological Research West of the Antarctic Peninsula. American Geophysical Union, Washington, DC, pp. 199-217.

Ross, R.M., Quetin, L.B., Haberman, K.L., 1998. Interannual and seasonal variability in short-term grazing impact of Euphasia superba in nearshore and offshore waters west of the Antarctic Peninsula. Jouranl of Marine Systems 17, 261-273.

Ryther, J., 1969. Photosynthesis and fish production in the sea. Science 166, 72-76.

Salihoglu, B., Fraser, W.R., Hofmann, E.E., 2001. Factors affecting fledging weight of Adelie penguin (*Pygoscelis adeliae*) chicks: a modeling study. Polar Biology 24, 328-337.

Smith, R.C., Baker, K.S., Byers, M.L., Stammerjohn, S.E., 1998. Primary Productivity of the Palmer Long Term Ecological Research Area and the Southern Ocean. Journal of Marine Systems 17, 245-259.

Ulanowicz, R.E., 1986. NETWRK3: A package of computer algorithms to analyze ecological flow networks, PASCAL implementation for the IBM-PC. University of Maryland Center for Environmental & Estuarine Studies, Solomons, MD.

Verity, P.G., Stoecker, D.K., Sieracki, M.E., Nelson, J.R., 1993. Grazing, growth and mortality of microzooplankton during the 1989 North Atlantic spring bloom at 47º N, 18º W. Deep-Sea Research I 40, 1793-1814.

Vezina, A.F., Pace, M.L., 1994. An inverse model analysis of planktonic food webs in experimental lakes. Canadian Journal of Fisheries and Aquatic Sciences 51, 2034-2044.

Vézina, A.F., Pahlow, M ., 2003. Reconstruction of ecosystem flows using inverse methods: how well do they work? Journal of Marine Systems 40-41, 55-77.

Vezina, A.F., Platt, T., 1988. Food web dynamics in the ocean. I. Best-estimates of flow networks using inverse methods. Marine Ecology Progress Series 42, 269-287.

Watson, A.J., Whitfield, M., 1985. Composition of particles in the global ocean. Deep-Sea Research 32, 1023-1039.

Wunsch, C., 1978. The north Atlantic general circulation west of 50ºW determined by inverse methods. Review of Geophysics and Space Physics 16, 583-620.

Wunsch, C., Minster, J.F., 1982. Methods for box models and ocean circulation tracers: mathematical programming and nonlinear inverse theory. Journal of Geophysical Research 87, 5647-5662.

APPENDICES

Appendix A. Mass balance equations, boundary conditions, and observation equations.

Flows are indicated as a 'C' for carbon followed by the compartment of origin (with a 3 letter designation), followed by 'TO', then followed by the destination compartment. Large phytoplankton gross production and small phytoplankton gross production are gpL and gpS, respectively.

Mass Balance Equations for NABE carbon model compartments.

Large Phytoplankton (phL): CgpLTOphL – CphLTOres – CphLTOmic – CphLTOmes – CphLTOdet – CphLTOdoc = 0 mmol $Cm^{-2}d^{-1}$

Small Phytoplankton (phS): CgpSTOphS – CphSTOres – CphSTOpro – CphSTOmic – CphSTOdet – CphSTOdoc = 0 mmol $Cm^{-2}d^{-1}$

Bacteria (bac): CdocTObac – CbacTOres – CbacTOpro – CbacTOmic – CbacTOdet = 6.3 mmol $Cm^{-2}d^{-1}$

Protozoans (pro): CbacTOpro + CphSTOpro + CdetTOpro – CproTOmic – CproTOmes – CproTOres – CproTOdet – CproTOdoc = 0 mmol $Cm^{-2}d^{-1}$

Microzooplankton (mic): CphLTOmic + CphSTOmic + CproTOmic + CbacTOmic + CdetTOmic – CmicTOres – CmicTOmes – CmicTOdet – CmicTOdoc = 9.2 mmol $Cm^{-2}d^{-1}$

Mesozooplankton (mes): CphLTOmes + CproTOmes + CmicTOmes + CdetTOmes – CmesTOres – CmesTOdet – CmesTOdoc – CmesTOext = 0 mmol $Cm^{-2}d^{-1}$

Detritus (det): CphLTOdet + CphSTOdet + CphSTOdet + CproTOdet + CmicTOdet + CmesTOdet + CbacTOdet – CdetTOpro – CdetTOmic – CdetTOmes – CdetTOdoc - CdetTOext = 0 mmol $Cm^{-2}d^{-1}$

DOC (doc): CphLTOdoc + CphSTOdoc + CproTOdoc + CmicTOdoc + CmesTOdoc + CbacTOdoc + CdetTOdoc – CdocTObac = 0 mmol $Cm^{-2}d^{-1}$

Boundary conditions for NABE carbon model.

Minimum Large Phytoplankton Primary Production: CgpLTOphL - CphLTOres - CphLTOdoc ≥ 31.5 mmol $Cm^{-2}d^{-1}$

Mazimum Large Phytoplankton Primary Production: CgpLTOphL - CphLTOres - CphLTOdoc ≤ 56.5 mmol $Cm^{-2}d^{-1}$

Minimum Small Phytoplankton Primary Production: CgpSTOphS – CphSTOres - CphSTOdoc ≥ 31.5 mmol $Cm^{-2}d^{-1}$

Maximum Small Phytoplankton Primary Production: CgpSTOphS - CphSTOres - CphSTOdoc ≤ 56.5 mmol $Cm^{-2}d^{-1}$

Minimum Export: CdetTOext ≥ 7.7 mmol $Cm^{-2}d^{-1}$

Maximum Export : CdetTOext ≤ 23.6 mmol $Cm^{-2}d^{-1}$

Observation equations for NABE carbon model.

Minimum Microzooplankton Grazing: CphLTOmic + CphSTOpro + CphSTOmic ≥ 40.5 mmol $Cm^{-2}d^{-1}$

Maximum Microzooplankton Grazing: CphLTOmic + CphSTOpro + CphSTOmic ≤ 121.5 mmol $Cm^{-2}d^{-1}$

Minimum Mesozooplankton Grazing: CphLTOmes ≥ 1.2 mmol $Cm^{-2}d^{-1}$

Maximum Mesozooplantkon Grazing: CphLTOmes ≤ 3.6 mmol $Cm^{-2}d^{-1}$

Minimum Bacterial Production: CbacTOpro + CbacTOmic + CbacTOdet ≤ 17.0 mmol $Cm^{-2}d^{-1}$

Maximum Bacterial Production: CbacTOpro + CbacTOmic + CbacTOdet ≥ 23.0 mmol $Cm^{-2}d^{-1}$

Mass Balance Equations for WAP 96 carbon inverse model. Large Phytoplankton (phL): CgpLTOphL – CphLTOres – CphLTOmic – CphLTOkri – CphLTOdet – CphLTOdoc = 0 mmol $Cm^{-2}d^{-1}$

Small Phytoplankton (phS): CgpSTOphS – CphSTOres – CphSTOpro – CphSTOmic – CphSTOdet – CphSTOdoc = 0 mmol $Cm^{-2}d^{-1}$

Bacteria (bac): CdocTObac - CbacTOres – CbacTOpro – CbacTOmic – CbacTOdet = 0 mmol $Cm^{-2}d^{-1}$

Protozoans (pro): CbacTOpro + CdetTOpro + CphSTOpro - CproTOmic – CproTOkri – CproTOres – CproTOdet – CproTOdoc = 0 mmol $Cm^{-2}d^{-1}$

Microzooplantkon (mic): CphLTOmic + CphSTOmic + CproTOmic + CbacTOmic + CdetTOmic + CbacTOmic + CdetTOmic – CmicTOres – CmicTOkri – CmicTOdet – CmicTOdoc = 0 mmol $Cm^{-2}d^{-1}$

Krill (kri): CphLTOkri + CproTOkri + CmicTOkri + CdetTOkri – CkriTOres – CkriTOdet – CkriTOdoc – CkriTOext = 0 mmol $Cm^{-2}d^{-1}$

Detritus: CphLTOdet + CphSTOdet + CproTOdet + CkriTOdet + CbacTOdet – CdetTOpro – CdetTOmic – CdetTOkri – CdetTOdoc – CdetTOext = 0 mmol $Cm^{-2}d^{-1}$

DOC (doc): CphLTOdoc + CphSTOdoc + CproTOdoc + CmicTOdoc + CkriTOdoc + CbacTOdoc + CdetTOdoc + CdocTObac = 0 mmol $Cm^{-2}d^{-1}$

Boundary conditions for WAP carbon model.

Minimum Large Phytoplankton Primary Production: CgpLTOphL – CphLTOres - CphlTOdoc ≥ 59.2 mmol $Cm^{-2}d^{-1}$

Maximum Large Phytoplankton Primary Production: CgpLTOphL – CphLTOres - CphlTOdoc ≤ 280.8 mmol $Cm^{-2}d^{-1}$

Minimum Small Phytoplankton Primary Production: CgpSTOphS – CphSTOres - CphsTOdoc ≥ 29.6 mmol $Cm^{-2}d^{-1}$

Maximum Small Phytoplankton Primary Production: CgpSTOphS – CphSTOres - CphsTOdoc ≤ 140.4 mmol $Cm^{-2}d^{-1}$

Minimum Export: CdetTOext ≤ 2.89 mmol $Cm^{-2}d^{-1}$

Maximum Export : CdetTOext ≥ 8.65 mmol $Cm^{-2}d^{-1}$

Observation equations for WAP carbon model.

Minimum Microzooplankton Grazing: CphLTOmic + CphSTOpro + CphSTOmic ≥ 0 mmol $Cm^{2}d^{-1}$

Maximum Microzooplankton Grazing: CphLTOmic + CphSTOpro + CphSTOmic ≤ 191.3 mmol $Cm^{-2}d^{-1}$

Minimum Krill Grazing: CphLTOkri ≥ 37.1 mmol $Cm^{-2}d^{-1}$

Maximum Krill Grazing: CphLTOkri ≤ 400.2 mmol $Cm^{-2}d^{-1}$

Minimum Bacterial Production: CbacTOpro + CbacTOmic + CbacTOdet ≥ 0 mmol $Cm^{-2}d^{-1}$

Maximum Bacterial Production: CbacTOpro + CbacTOmic + CbacTOdet ≤ 127.5 mmol $Cm^{-2}d^{-1}$

Appendix B. Biological constraints for inverse models.

Where constraints are different between the WAP and NABE models, the components are listed separately. The temperature, T is equal to 15º C for NABE and -2º C for the WAP. Mbac = pmol of C/bacteria cell, Cbacteria = biomass of bacteria in mmol Cm^{-2}, MicC = pmol of C/microzooplankton cell, Cmicro = biomass of microzooplankton in mmol Cm^{-2}, MesC = pmol of C/individual, Cmesozoo = biomass of mesozooplankton in mmol Cm^{-2}. KrillC = pmol of C/individual, Ckrill = biomass of mesozooplankton in mmol Cm^{-2}.

Biological Constraints	Lower Bound	Upper Bound	Reference
Respiration			
Bacteria	20 % of consumption of DOC	(1.7*(Mbac)^-0.25*EXP(0.0693*(T-20)))*Cbacteria	1,2
Large Phytoplankton	5 % of GPP	30 % of gross primary production	2
Small Phytoplankton	5 % of GPP	30 % of gross primary production	2
Protozoa	20 % of total C intake	None	2
Microzooplankton (NABE)	20 % of total C intake	(14*('MicC')^-0.25*EXP(0.0693*(T-20)))*'Cmicro'	1,2
Microzooplankton (WAP)	20 % of total C intake	None	1,2
Mesozooplankton (NABE)	20 % of total C intake	(14*(mesoC)^-0.25*EXP(0.0693*(T-20)))*Cmeso	1,2
Krill (WAP)	20 % of total C intake	(14*(krillC)^-0.25*EXP(0.0693*(T-20)))*Ckrill	1,2
Excretion			
Large Phytoplankton	2 % of large phytoplankton NPP	55 % of large phytoplankton NPP	3
Small Phytoplankton	2 % of small phytoplankton NPP	55 % of small phytoplankton NPP	3
Protozoa	10 % of total C intake	100 % of protozoan respiration	4
Microzooplankton	10 % of total C intake	100 % of microzooplankton respiration	4
Mesozooplankton (NABE)	10 % of total C intake	100 % of mesozooplankton respiration	4
Krill (WAP)	10 % of total C intake	100 % of krill respiration	4
Assimilation efficiency			
Protozoa	C output to Detritus <= 50% of total C intake	C output to Detritus >= 10% of total C intake	2
Microzooplankton	C output to Detritus <= 50% of total C intake	C output to Detritus >= 10% of total C intake	2
Mesozooplankton (NABE)	C output to Detritus <= 50% of total C intake	C output to Detritus >= 10% of total C intake	2

Biological Constraints Continued	Lower Bound	Upper Bound	Reference
Assimilation efficiency			
Krill (WAP)	C output to Detritus <= 28% of total C intake	C output to Detritus >= 6% of total C intake	5
Net production efficiency			
Bacteria	bacteria to DOC + bacterial respiration <= 95% DOC to bacteria	bacteria to DOC + bacterial respiration >= 50% DOC to bacteria	2
Gross production efficiency			
Protozoa	losses to respiration + detritus + DOC <= 90 % of total carbon intake	losses to respiration + detritus + DOC >= 60 % of total carbon intake	2
Microzooplankton	losses to respiration + detritus + DOC <= 90 % of total carbon intake	losses to respiration + detritus + DOC >= 60 % of total carbon intake	2
Mesozooplankton (NABE)	losses to respiration + detritus + DOC <= 90 % of total carbon intake	losses to respiration + detritus + DOC >= 60 % of total carbon intake	
Krill (WAP)	losses to respiration + detritus + DOC <= 90 % of total carbon intake	losses to respiration + detritus + DOC >= 60 % of total carbon intake	2
Ingestion			
Bacteria	None	(3.6*(Mbac)^-0.25*EXP(0.0693*(T-20)))*Cbacteria	1,2
Mesozooplankton (NABE)	None	(63*(mesC)^-0.25*EXP(0.0693*(T-20)))*Cmesozoo	1,2
Krill (WAP)	None	(63*(krill C)^-0.25*EXP(0.0693*(T-20)))*Ckrill	1,2

References. 1. Moloney & Field (1989) 2. Vezina & Platt (1989) 3. Baines and Pace (1991) 4. Vezina and Pace (1994) 5. Kato (1982)

Table 1. Data input to the North Atlantic Bloom (NABE) and Western Antarctic Peninsula (WAP) models including rate processes and biomasses. NABE entries represent statistics for the May 18-31 time series (Figure 3).WAP entries are for all January observations within the Adélie penguin foraging territory. The data for NABE and for the WAP were all integrated to 35 m for comparison between the two environments (see text for details)

	NABE 1989				WAP 1996			
	AVG	**St Dev**	**Min**	**Max**	**AVG**	**St Dev**	**Min**	**Max**
RATES (mmol C $m^{-2}d^{-1}$)								
Phyto-plankton Production	88	25	63	113	254	166	88	420
Small Phyto-plankton Production	44	12.5	31.5	56.5	84.8	55.4	29.4	140
Large Phyto-plankton Production	44.0	12.5	31.5	56.5	169.7	110.8	58.9	280.5
Bacterial Productivity	19.8	6.4	13.4	26.3	–	–	0	50 % of PP
Microzoo-Plankton Grazing	81.3	–	40.6	121.9	–	–	0	75 % of PP
Mesozoo-plankton Grazing	2.4	–	1.0	3.0	–	–	37.1	400.2

Table 1. (continued)

	NABE 1989				WAP 1996			
	AVG	**St Dev**	**Min**	**Max**	**AVG**	**St Dev**	**Min**	**Max**
Export	15.7	–	7.7	23.6	5.77	–	2.88	8.66
BIOMASS (mmol C m^{-2})								
Phyto-plankton	423.1	111.3	–	–	1437.8	1007.7	–	–
Bacteria	86.1	33.1	–	–	10.09	5.70	–	–
Microzoo-plankton	91.0	46.0	–	–	–	–	–	–
Mesozoo-plankton or Krill (WAP)	7.4	6.0	–	–	2672	–	–	–

Table 2. Comparison of the 1989 North Atlantic carbon inverse solution and the 1996 Western Antarctic Peninsula carbon solution

Flow #	Food Web Flow	WAP Flows (mmol $Cm^{-2}d^{-1}$)	NABE Flows (mmol $Cm^{-2}d^{-1}$)	WAP Flows (% of PP)	NABE Flows (% of PP)
1	Large phytoplankton gross primary production	65.9	34.5	70	55
2	Large phytoplankton respiration	3.3	1.7	4	3
3	Microzooplankton grazing of large phytoplankton	12.8	16.1	14	26
4	Krill or mesozooplankton grazing of large phytoplankton	37.1	3.6	40	6
5	Large phytoplankton to detritus	9.3	11.9	10	19
6	Large phytoplankton release of DOC	3.4	1.3	4	2
7	Small phytoplankton gross primary production	32.9	34.5	35	55
8	Small phytoplankton respiration	1.6	1.7	2	3
9	Protozoan grazing of small phytoplankton	13.3	13.1	14	21
10	Microzooplankton grazing of small phytoplankton	9.9	11.3	11	18
11	Small phytoplankton to detritus	6.4	7.1	7	11
12	Small phytoplankton release of DOC	1.7	1.3	2	2
13	Microzooplankton consumption of protozoans	0.8	0.9	1	1
14	Krill or mesozooplankton consumption of protozoans	1.3	1.0	1	2
15	Protozoan respiration	14.6	7.6	16	12
16	Protozoans to detritus	2.1	1.9	2	3

Table 2. (continued)

Flow #	Food Web Flow	WAP Flow (mmol $Cm^{-2}d^{-1}$)	NABE Flow (mmol $Cm^{-2}d^{-1}$)	WAP Flows (% of PP)	NABE Flows (% of PP)
17	Protozoans to DOC	2.1	7.6	2	12
18	Microzooplankton respiration	19.0	9.8	20	16
19	Krill or mesozooplankton consumption of microzooplankton	2.7	0.2	2.9	0
20	Microzooplankton to detritus	2.7	3.2	2.9	5
21	Microzooplankton to DOC	2.7	9.8	2.9	16
22	Krill or mesozooplankton respiration	19.9	1.2	21	2
23	Krill or mesozooplankton to detritus (Faecal pellets)	2.7	2.0	3	3
24	Krill or mesozooplankton to DOC	4.5	1.2	5	2
25	Bacterial respiration	13.7	11.7	15	19
26	Bacteria to protozoans	0.7	5.8	1	9
27	Bacteria to microzooplankton	0.0	4	0	6
28	Bacteria to detritus	0.0	7.2	0	11
29	Protozoan consumption of detritus	6.9	0	7	0
30	Microzooplankton consumption of detritus	3.5	0	4	0
31	Krill or mesozooplankton consumption of detritus	4.1	0	4	0
32	Detritus to DOC	0.0	25.5	0	40

Table 2. (continued)

Flow #	Food Web Flow	WAP Flows (mmol $Cm^{-2}d^{-1}$)	NABE Flows (mmol $Cm^{-2}d^{-1}$)	WAP Flows (% of PP)	NABE Flows (% of PP)
33	Bacterial carbon demand	14.4	46.7	15	74
34	Total Particulate Export out of the top 35 m	8.7	7.7	9	12
35	Krill or mesozooplankton to export (Consumption by higher trophic levels or mortality)	18.1	0.5	19	1

Table 3. Comparison of the microbial and short food web flows for the WAP and the NABE carbon models.

Microbial Food Web Flows	WAP (% of PP)	NABE (% of PP)
S Phytoplankton to Detritus	6.8	11.2
S Phytoplankton to DOC	1.8	2.1
Protozoan Grazing of S Phytoplankton	14.1	20.8
Protozoan Grazing of Bacteria	0.8	9.2
Microzooplankton Grazing of Bacteria	0.0	6.3
Microzooplankton Grazing of L Phytoplankton	13.7	25.5
Microzooplankton Grazing of S Phytoplankton	10.6	17.9
Microzooplankton Grazing of Protozoans	15.4	1.4
Bacterial Carbon Demand	2.2	74.1
Bacteria to Detritus	0.0	11.4
Protozoan to Detritus	2.2	3.0
Protozoans to DOC	2.2	12.0
Microzooplankton to DOC	2.9	15.6
Detritus to DOC	0.0	40.5
Detritus to Protozoans	7.3	0.0
Detritus to Microzooplankton	3.8	0.0
Microzooplankton to Detritus	2.9	5.1
Total	86.6	256.2

Table 3 (continued).

Short Food Web Flows	**WAP (% of PP)**	**NABE (% of PP)**
L Phytoplankton to Detritus	9.9	18.8
Krill Grazing of L Phytoplankton	39.5	5.7
Other Krill Production	19.3	0.8
Krill Faecal pellets	2.9	3.1
Total	71.6	28.4
Microbial Food Web Flows / Short Food Web Flows	1.2	9.0

Table 4. Network analysis indices for the WAP 1996 condensed carbon model and the NABE carbon model.

	WAP	**NABE**
Fbac (%)	1	26
Fpro (%)	22	41
Fmic (%)	29	49
Fkri or Fmes (%)	49	10
L	1.5	3.0
Total Ingestion / PP	1.15	1.6

Table 5. Effective trophic levels of components in the NABE and WAP carbon models

Component	Effective Trophic Level	
	NABE	**WAP**
Small Phytoplankton	1	1
Large Phytoplankton	1	1
Protozoans	2.31	2.03
Microzooplankton	2.16	2.03
Mesozooplankton / Krill	2.32	2.09
Bacteria	2	2
DOC	1	1
Detritus	1	1

Table 6. Comparison of food web classifications of the Inverse Model results with the 5 different food web types described by Legendre & Rassoulzadegan (1996)

Biogenic carbon pathways (Legendre & Rassoulzadegan, 1996)	**P_L/P_T**	**M**	**R_T/P_T**	**F_T/P_T**	**D_T/P_T**
(1) Sinking of ungrazed cells	1.00	0.00	0.00	0.00	1.00
(2) Herbivorous food web	0.80	0.55	0.30	0.60	0.10
(3) Multivorous food web	0.35	0.65	0.60	0.30	0.10
(4) Microbial food web	0.10	0.25 or 0.75	0.80	0.20	0.00
(5) Microbial loop	0.00	0 or 1	1.00	0.00	0.00
Inverse Models					
NABE Carbon	0.50	–	0.84	0.04	0.12
WAP 1996 Carbon	0.67	–	0.69	0.22	0.09

FIGURE LEGENDS

Figure 1. Inverse solution food web diagrams for (**a**) NABE and (**b**) the WAP. The width of the arrow is proportional to the magnitude of the flow. Gray arrows leaving compartments are losses to respiration. Inputs are from gross primary production for small phytoplankton (gpS) and large phytoplankton (gpL). Export from the surface ocean enters the ext compartment. Black arrows are allowed (potential) flows that were zero in the solutions.

Figure 2. NABE measurements at 47˚ N 20˚ W during May, 1989 aboard the Atlantis II; (**a**) primary production; (**b**) phytoplankton biomass; (**c**) bacterial production; (**d**) bacterial biomass; (**e**) microzooplankton grazing; (**f**) microzooplankton biomass, (**g**) mesozooplankton grazing and (**h**) mesozooplankton biomass.

Figure 3. Adélie penguin foraging areas for 1996 and 1999 within the Palmer LTER regional grid that is sampled during the annual January cruise. The grid lines are every 100 km along the coast of the western Antarctic Peninsula, and the stations are every 20 km along a grid line extending 200 km offshore. The foraging areas are the seaward portions of the circles centered at Anvers Island. Measurements at stations within the 1996 foraging area were averaged and used as inputs to the model.

Figure 4. 1996 WAP measurements from Palmer Station near shore station E and from the January regional cruises, including (**a**) primary production, (**b**) phytoplankton biomass, and (**c**) bacterial biomass.

Figure 5. Contributions to the DOC pools in (**a**) the NABE carbon inverse solution and (**b**) the WAP carbon inverse solution as a % of the total flows entering.

Figure 6. Sensitivity analysis for the NABE model. (**a**) effects on the food web flows from varying the large and small phytoplankton production by +/- 10%. The food web flows can be identified by number in Table 2. (**b**) effects on the flows from varying the microzooplankton grazing and bacterial production. Solid lines: Input large phytoplankton production increased 10%. Dashed lines: Input large phytoplankton production decreased 10%. Dotted lines: Input small phytoplankton production increased 10%. Dash-dotted lines: Input small phytoplankton production decreased 10%.

Figure 7. Sensitivity analysis for the WAP model. (**a**) effects on the food web flows from varying the large and small phytoplankton production by +/- 10%. The food web flows can be identified by number in Table 2. (**b**) effects on the flows from varying the minimum bacterial production constraint by +/- 10% and the krill minimum grazing constraint by +/- 10%. Solid lines: Input minimum bacterial production increased 10%. Dashed lines: Input minimum krill grazing decreased 10%. Dotted lines: Input krill grazing decreased 10%.

a

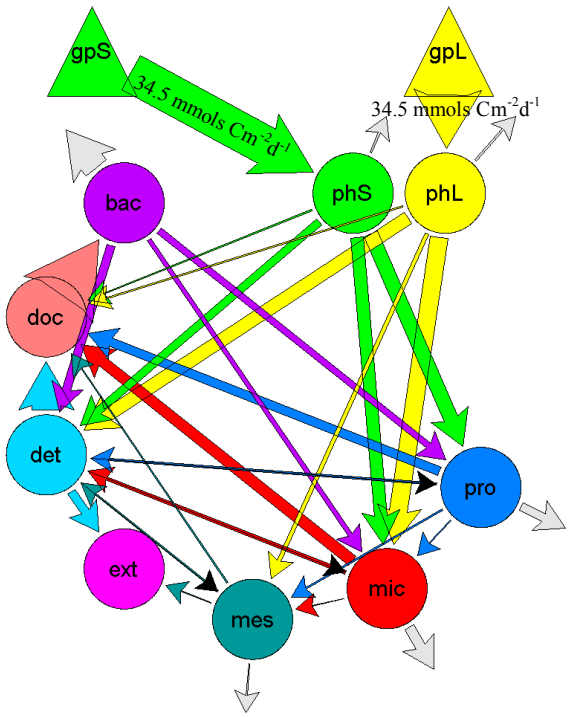

b

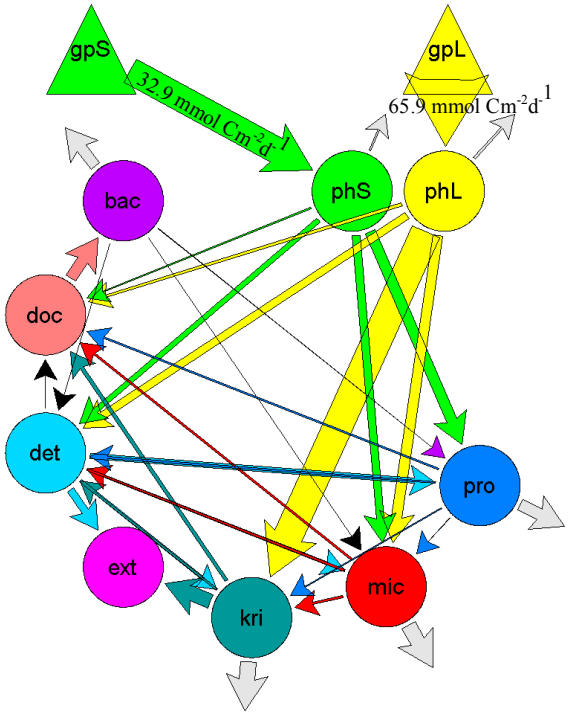

gpS = Gross PP for Small Phytoplankton

gpL = Gross PP for Large Phytoplankton

bac = Bacteria

det = Detritus

ext = External

mes = Mesozooplankton

kri = Krill

mic = Microzooplankton

pro = Protozoans

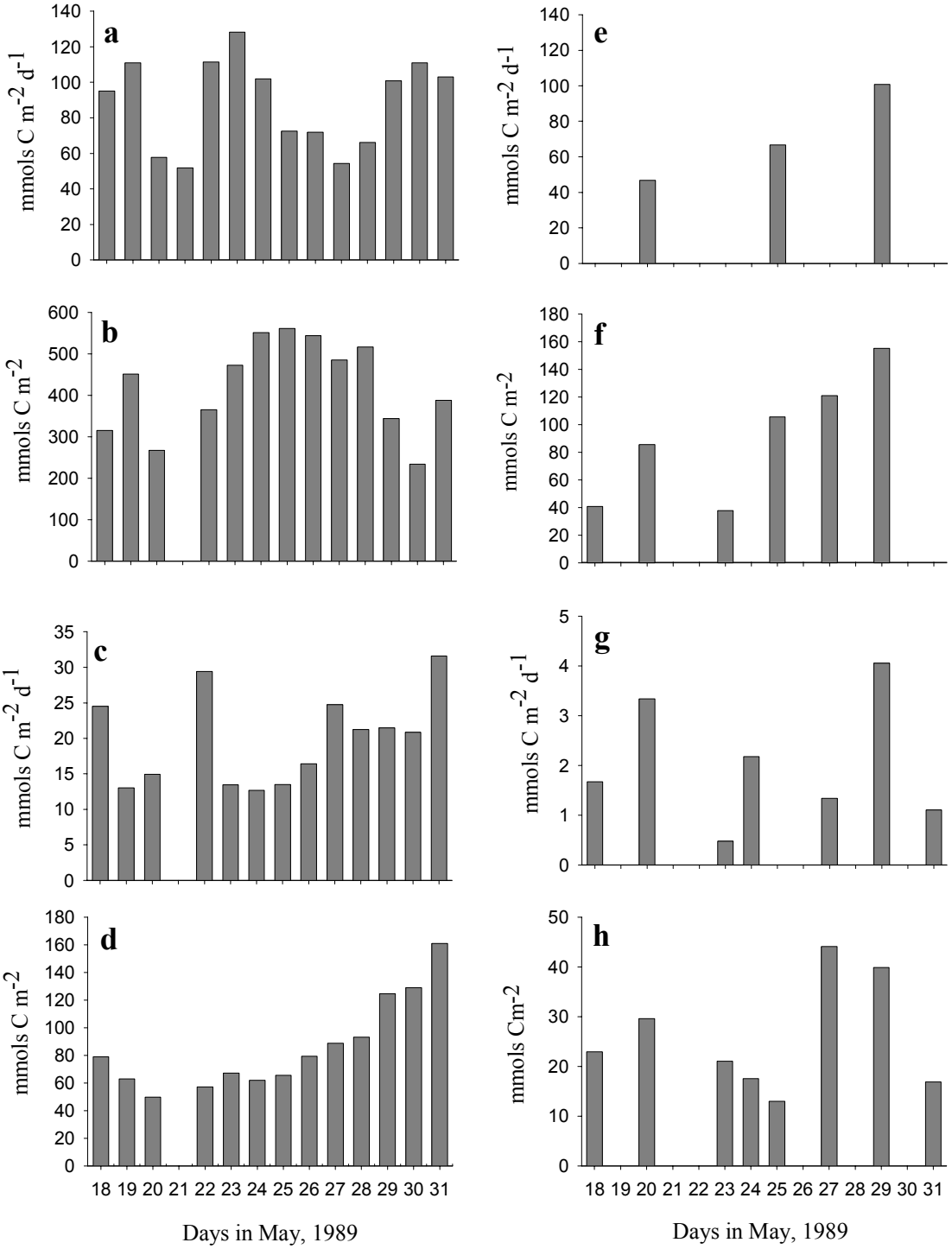

Figure 2 Daniels and Ducklow

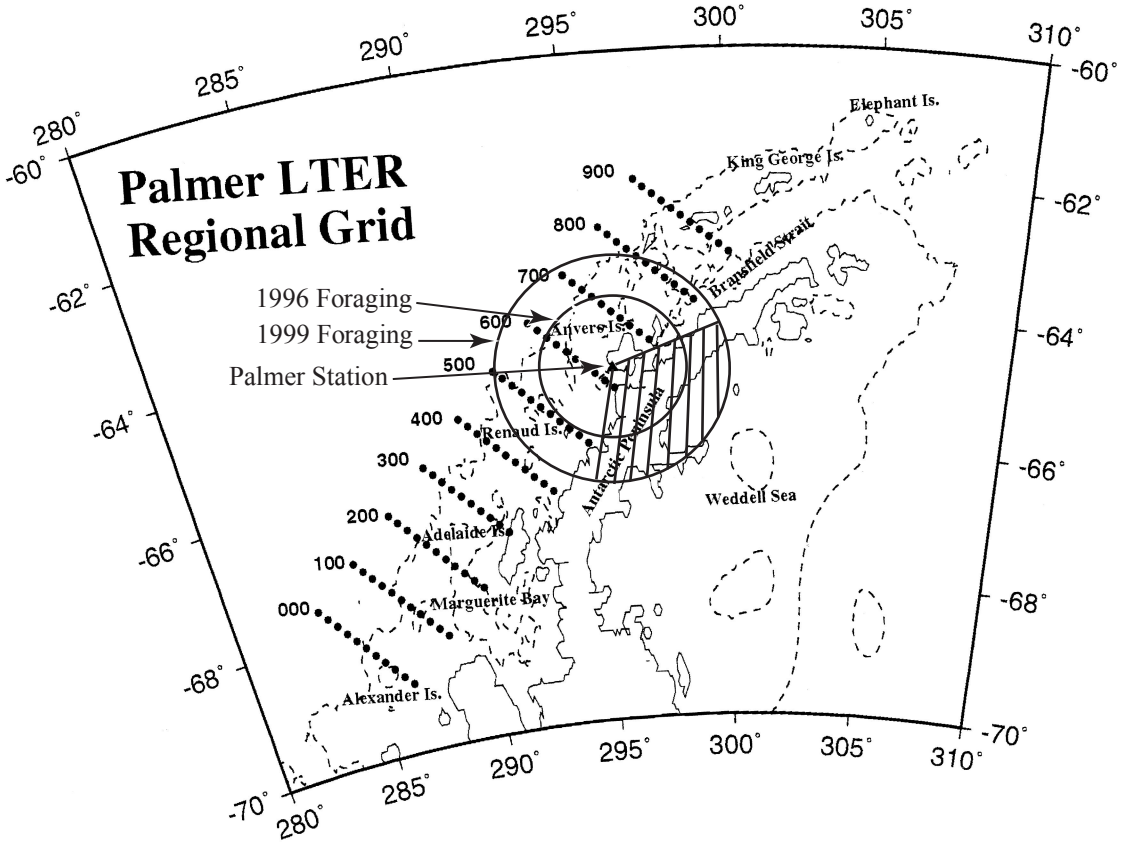
Palmer LTER
Regional Grid
1996 Foraging
1999 Foraging
Palmer Station
Elephant Is.
King George Is.
Bransfield Strait
Anvers Is.
Renaud Is.
Antarctic Peninsula
Weddell Sea
Adelaide Is.
Marguerite Bay
Alexander Is.
900
800
700
600
500
400
300
200
100
000
280°
285°
290°
295°
300°
305°
310°
-60°
-62°
-64°
-66°
-68°
-70°

Figure 4 Daniels and Ducklow

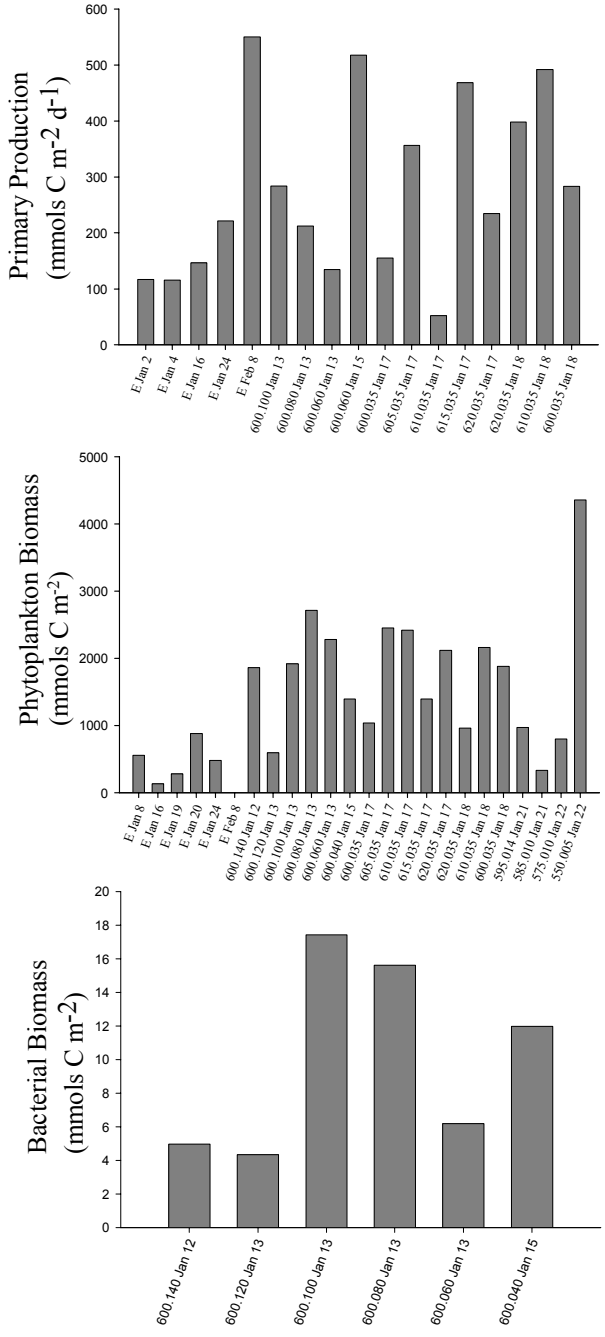

Figure 5 Daniels and Ducklow

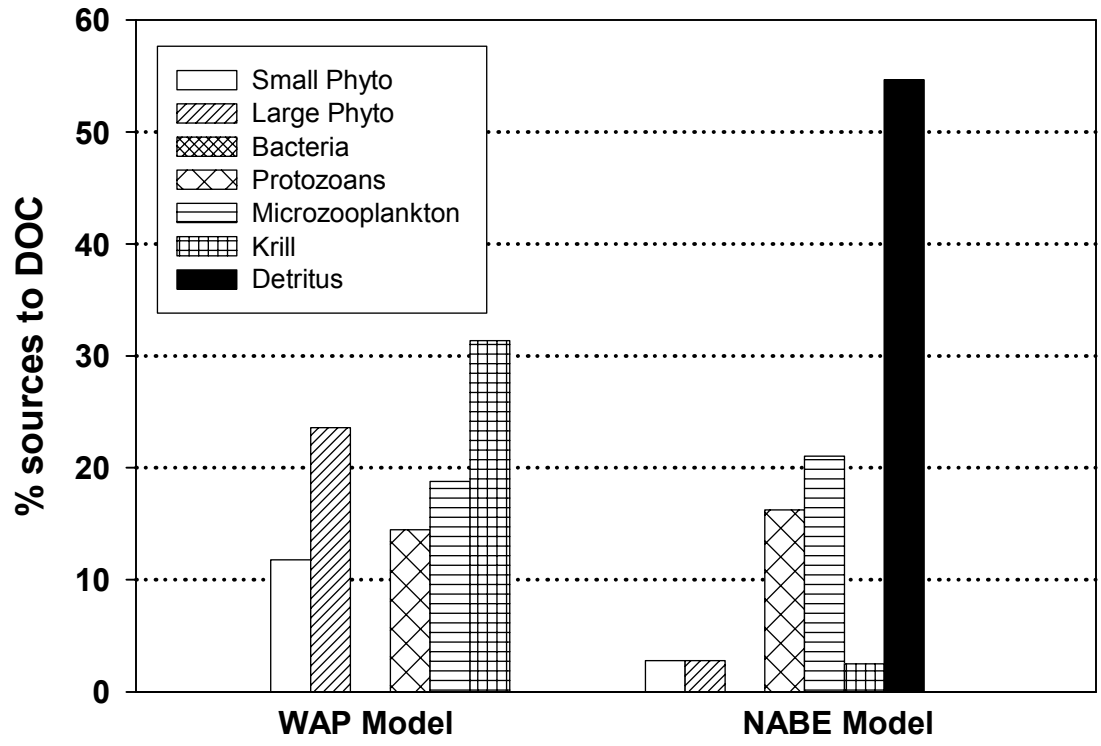

Figure 6 Daniels and Ducklow

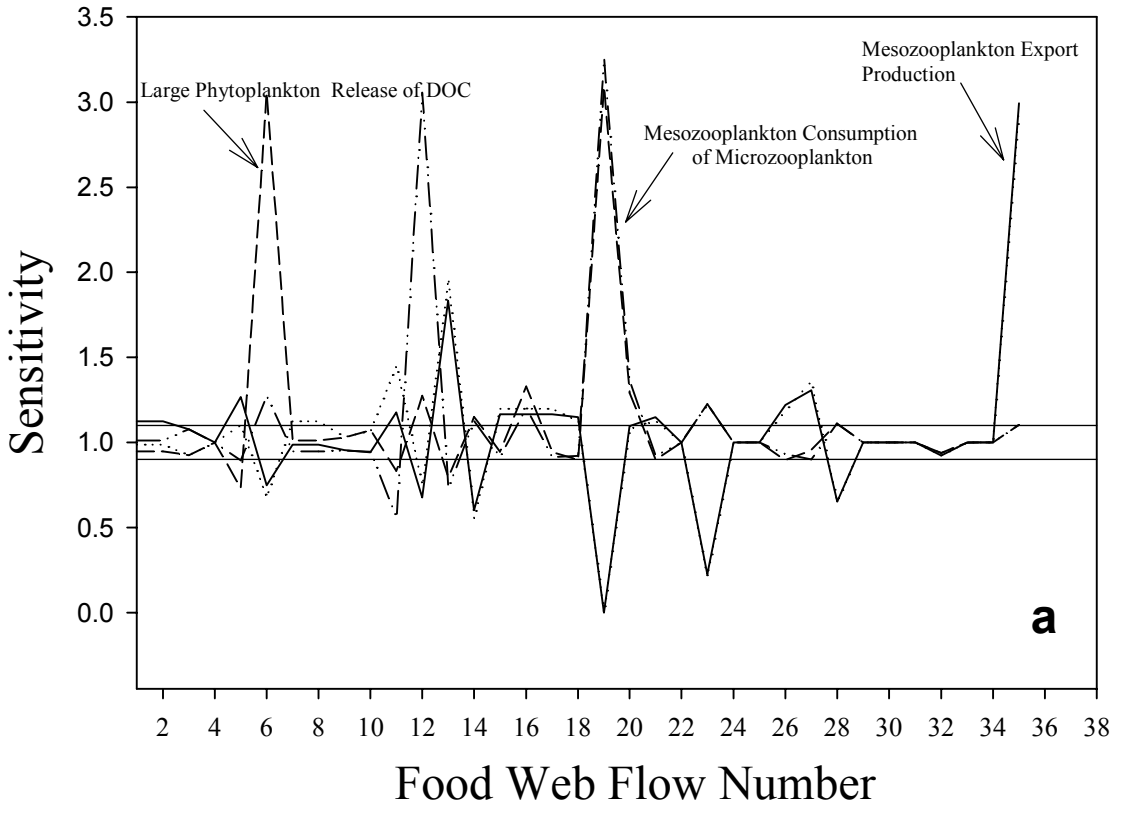

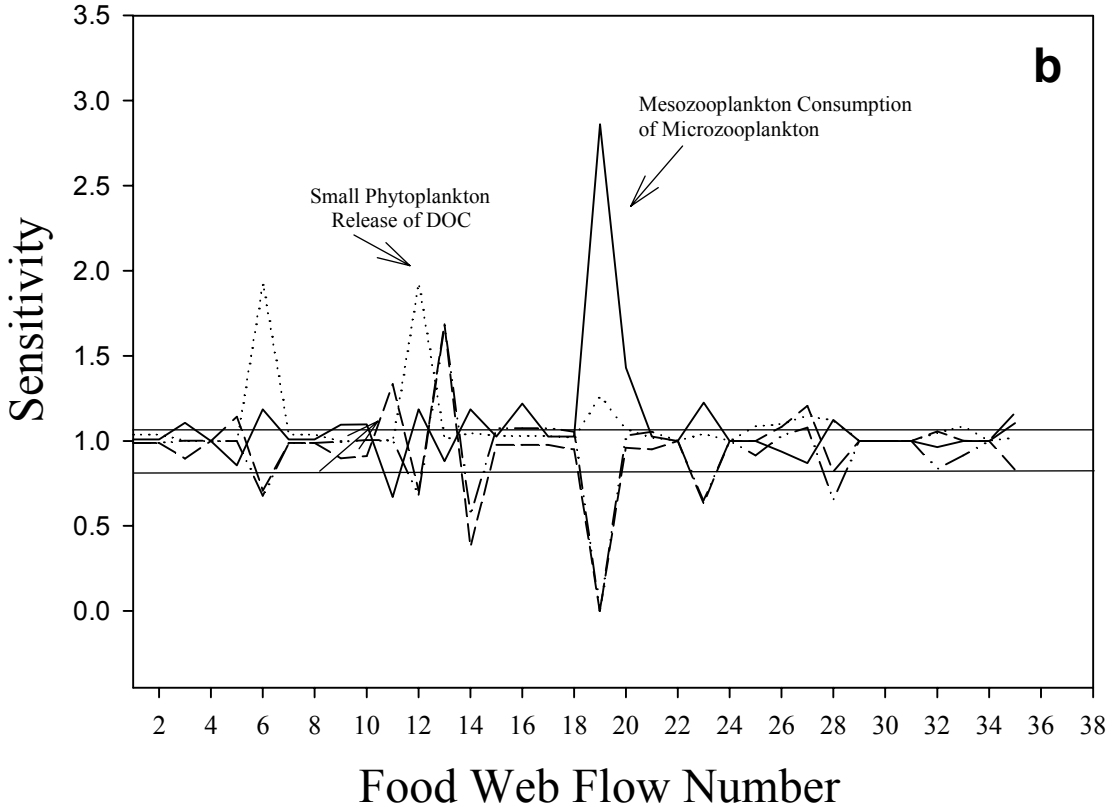

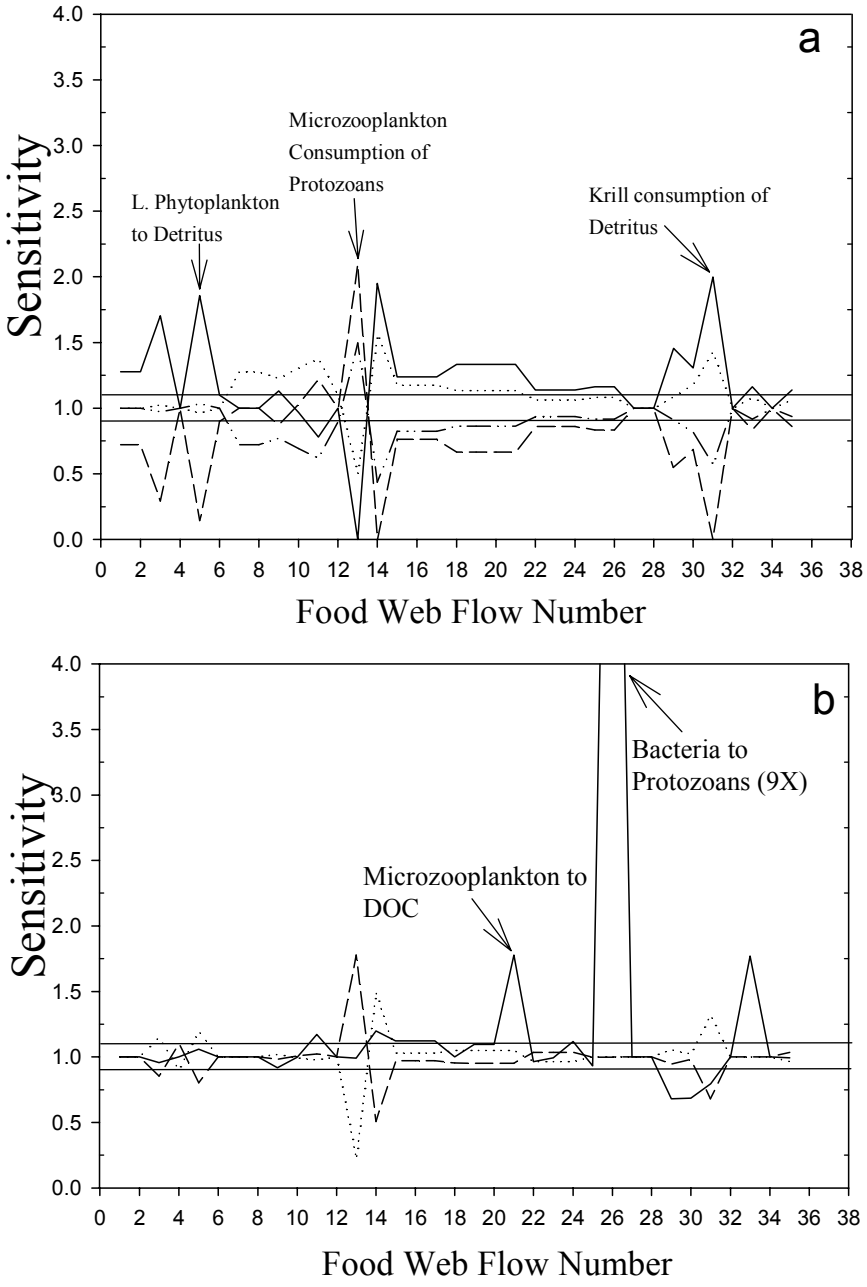

Figure 7 Daniels and Ducklow